National Tsing Hua University

2016-2017

R&D REPORT

Plan to Develop World-Class Universities
and Top-Notch Research Centers

A Brief History of NTHU

National Tsing Hua University (NTHU) was established in Beijing in 1911 as "Tsing Hua Academy." The Academy was renamed as "National Tsing Hua University" in 1928. In 1956, NTHU was re-established at its present location in Hsinchu, Taiwan.

Since its relocation, NTHU has developed into a comprehensive research university offering a full range of degree programs in science, technology, engineering, humanities, social sciences, and management. NTHU has been consistently ranked as one of the premier universities in East Asia, and is widely recognized as a leading incubator for future leaders. Our outstanding alumni highlight the success of NTHU students, including Nobel Physics laureates Dr. Cheng-Ning Yang and Dr. Tsung-Dao Lee, Nobel Chemistry laureate Dr. Yuan-Tseh Lee, and Wolf Prize winner in mathematics Dr.Shiing-Shen Chern.

Contents

Message from the President

National Tsing Hua University (NTHU) is a research university with a long and proud tradition. Since the re-establishment in Hsinchu in 1956, NTHU has been known for excellent academic programs as well as outstanding alumni. Over the last sixty years, NTHU has transformed herself into a comprehensive university and is recognized in all disciplines.

NTHU provides a stimulating and nurturing environment within which our faculty can offer quality teaching and conduct innovative research. Regarded as one of the top-tier research universities, our research and development activities across the University emphasize fundamental discoveries at the forefronts of basic sciences and exploration of breakthrough technologies with a high potential for applications. These can be reflected from our publications in the world's preeminent journals, awarded international patents, and technology transfer cases. In the 2016-2017 R&D annual report, we highlight several key papers published in Scientific Breakthrough. We also provide the facts and figures related to other important R&D activities, including a coverage of the research centers jointly established with the leading corporates in Taiwan. This volume is undoubtedly too limited to give the full scope of R&D at NTHU, but a glimpse into our recent achievements. Hopefully, this can serve as a catalyst for further interactions, exchange of ideas, and establishment of collaborations.

Built on our proud heritage, NTHU will continue to promote excellent teaching and innovative research with the goal of ascending the University into the cradle of human accomplishments, important scientific discoveries and innovative technologies. I hope that you will find this R&D annual report useful and give us your precious opinions and suggestions.

President
Dr. Hong Hocheng

National Tsing Hua University
Hsinchu, Taiwan
November 2017

NTHU Today

Location

National Tsing Hua University is located in Hsinchu, a city 72 kilometers south of Taipei. The campus covers an area of over 136.06 hectares (366.2 acres) scenic land with lakes and trees. The campus has a convenient access to neighboring industrial sectors, research institutes and universities such as the Hsinchu Science Park (HSP), the Industrial Technology Research Institute (ITRI), National Synchrotron Radiation Research Center (NSRRC), National Center for High-Performance Computing (NCHC), Food Industry Research and Development Institute (FIRDI), National Chiao Tung University (NCTU), Chung Hua University (CHU), and National Hsinchu University of Education (NHCUE). These establishments have made Hsinchu known as "The Science City of Taiwan".

Academics

10 Colleges, 26 Departments and 27 Institutes

- College of Science
- College of Engineering
- College of Technology Management
- College of Humanities and Social Sciences
- College of Life Science
- College of Nuclear Science
- College of Electrical Engineering and Computer Science
- Hsinchu Teachers College
- College of Arts
- Tsing Hua College

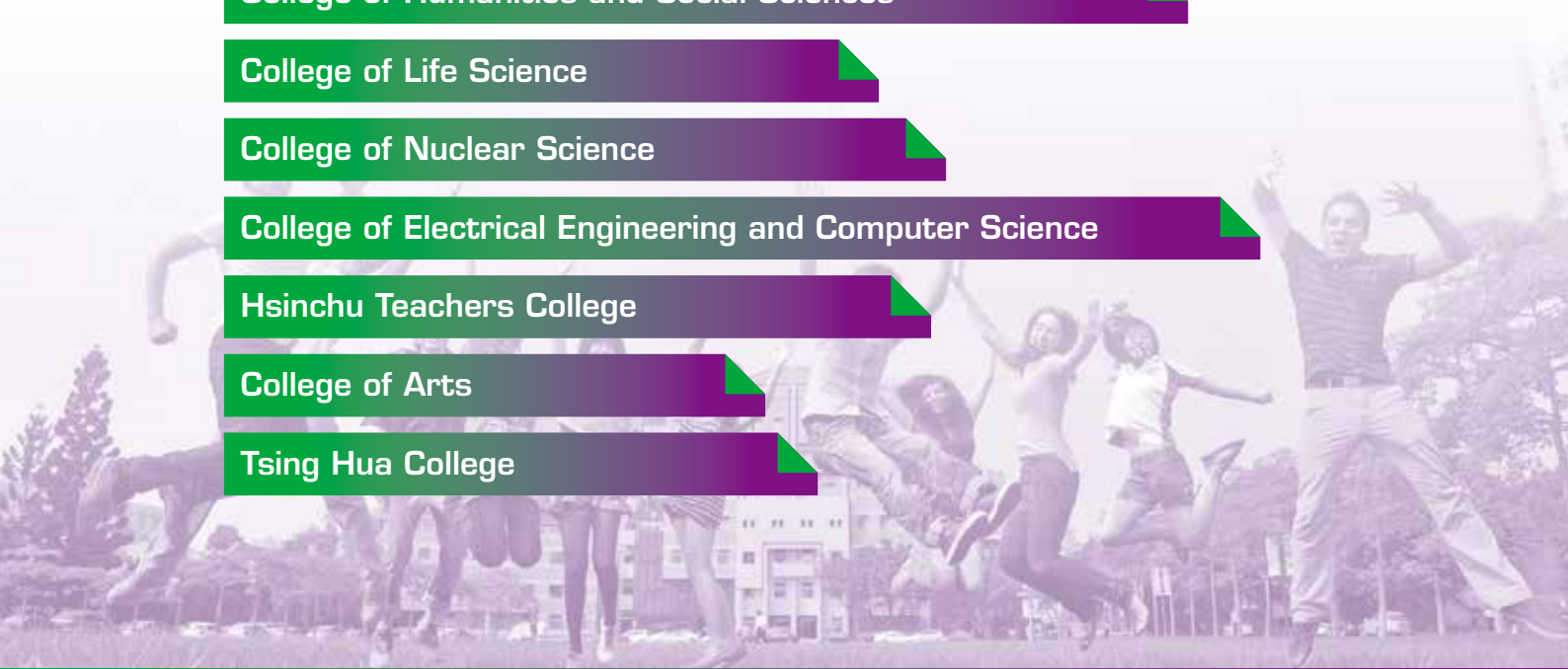

Colleges & Degree Programs

B:Baccalaureate / M:Master / D:Doctorate
P:Degree Program / X:Post Graduate

College of Science	Academoc Degee
Department of Mathematics	B / M / D
Department of Physics	B / M / D
Department of Chemistry	B / M / D
Interdisciplinary Program of Science	B
Institute of Statistics	M / D
Institute of Astronomy	M / D
Graduate Program in Science and Technology of Synchrotron Light Source	M / D
Institute of Computational and Modeling Science	M

College of Engineering	Academoc Degee
Department of Chemical Engineering	B / M / D
Department of Power Mechanical Engineering	B / M / D
Department of Materials Science and Engineering	B / M / D
Department of Industrial Engineering and Engineering Management	B / M / D / P
Interdisciplinary Program of Engineering	B
Institute of Nano Engineering and MicroSystems	M / D
Institute of Biomedical Engineering	M
Dual Master Program for Global Operation Management	M
Ph.d. Program in Prospective Functional Materials Industry	D

College of Technology Management	Academoc Degee
Department of Quantitative Finance	B / M / D
Department of Economics	B / M / D
Double Specialty Program of Management and Technology	B
Institute of Technology Management	M / D
Institute of Law for Science and Technology	M / D / X
Institute of Service Science	M / D
International Master of Business Administration (IMBA)	M
Master of Business Administration (MBA)	P
Executive Master of Business Administration (EMBA)	P
Master Program of Finance and Banking (MFB)	P
Master Program of Public Policy and Management (MPM)	P

College of Humanities and Social Sciences	Academoc Degee
Department of Chinese Literature	B / M / D
Department of Foreign Languages and Literature	B / M
Interdisciplinary Program of Humanities and Social Sciences	B
Institute of History	M / D
Institute of Linguistics	M / D
Institute of Anthropology	M / D
Institute of Sociology	M / D
Institute of Philosophy	M
Institute of Taiwan Literature	M / D
Institute of Sinophone Studies	M
Graduated Program of Taiwan Studies for in-service Teachers	P
International Undergraduate Program of College of Humanities and Social Sciences	B
International Master's Program in Inter-Asia Cultural Studies	M

College of Life Science	Academoc Degee
Department of Life Science	B
Department of Medical Science	B
Interdisciplinary Program of Life Science	B
Institute of Molecular Medicine	M / D
Institute of Molecular and Cellular Biology	M / D
Institute of Biotechnology	M / D
Institute of Bioinformatics and Structural Biology	M / D
Institute of Systems Neuroscience	M / D
Ph.D. Program in Bioindustrial Technology	D
Internaional Ph.D. Program in Interdisciplinary Neuroscience	D

College of Nucclear Science	Academoc Degee
Department of Engineering and System Science	B / M / D
Department of Biomedical Engineering and Environmental Sciences	B / M / D
Interdisciplinary Program of Nuclear Science	B
Institute of Nuclear Engineering and Science	M / D
Internaional Ph.D. Program in Environmental Science and Technology	D

College of Electrical Engineering and Computer Science	Academoc Degee
Department of Computer Science	B / M / D
Department of Electrical Engineering	B / M / D
Undergraduate Program of Electrical Engineering and Computer Science	B
Institute of Communications Engineering	M / D
Institute of Electronics Engineering	M / D
Institute of Information Systems and Applications	M / D
Institute of Photonics Technologies	M / D
Internaional Ph.D. Program in Photonics	D

Hsinchu Teachers College	Academoc Degee
Department of Education and Learning Technology	B / M / D / P
Department of Early Childhood Education	B / M / P
Department of Special Education	B / M
Department of Educational Psychology and Counseling	B / M / D / P
Department of Physical Education	B / M / P
Department of English Instruction	B / M
Department of Environmental and Cultural Resources	B / M / P
Interdisciplinary Program of Hsinchu Teachers College	B
Graduate Institute of Mathematics and Science Education	M / P
Institute of Taiwan Languages and Language Teaching	M / D
Institute of Learning Sciences and Technologies	M

College of Arts	Academoc Degee
Department of Music	B / M
Department of Arts and Design	B / M / P
Interdisciplinary Program of Arts College	B

Tsing Hua College	Academoc Degee
Tsing Hua College Interdisciplinary Program	B

Office of Academic Affairs	Academoc Degee
International Intercollegiate Program	M / D

Personnel

Based on April 2017 Figure

Faculty	Title	Total
Full-Time(630)	Professor	418
	Associate Professor	255
	Assistant Professor	114
	Instructor	4
	Military Instructor	8
Research Fellow		240
Faculty on Term Appointment		31
Adjunct Professor		541

Staff	Total
Regular	248
Campus Police	21
Term Appointment	558
Research Staff (Funded by Projects)	541

Number of students, as of March 2017

Total: 15,945

International students

Graduates, as of 2016

Total: 3,222

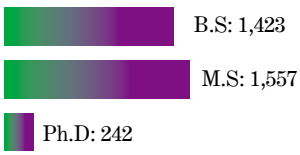

R & D Facts and Figures

Research Funding (2003-2015)

Industry & Others Government

Unit:Million NTD
30 NTD ≈ 1 USD

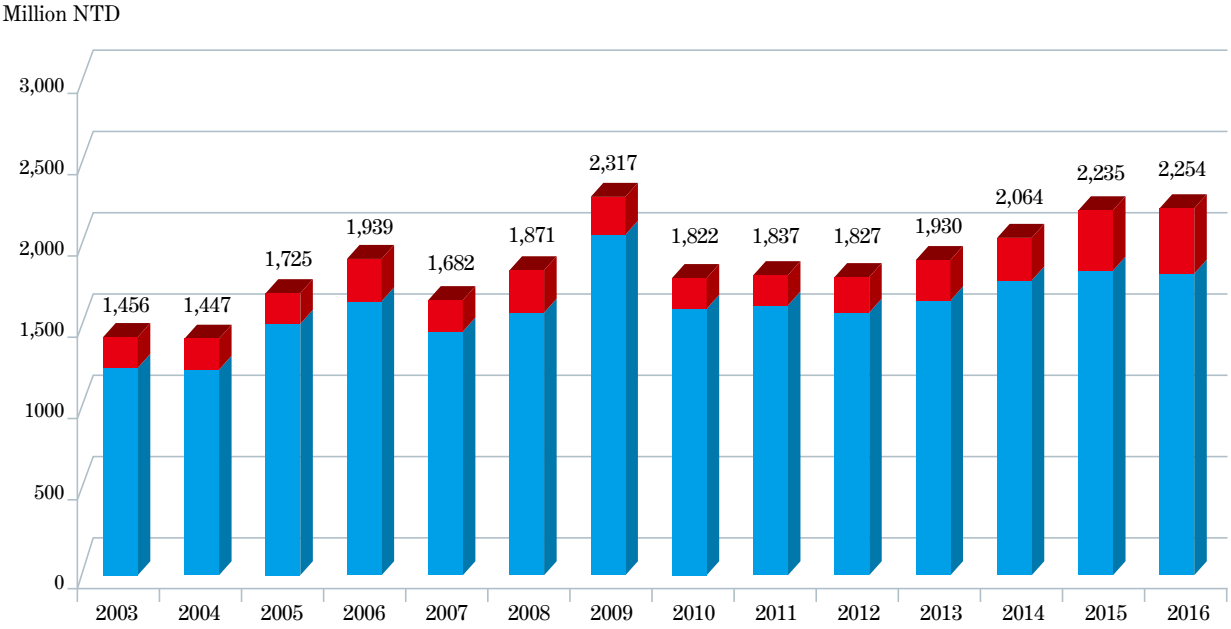

Funding Distribution by Discipline (2016)

Unit: Million NTD (30 NTD ≈ 1 USD)

Physical Sciences	438	15%
Engineering	1,307	44%
Social Sciences	153	5%
Life Sciences	224	8%
Arts & Humanities	78	3%
Clinical, Pre-Clinical & Health	729	25%

Sponsored Research Fund (2016)

Unit: Million NTD (30 NTD ≈ 1 USD)

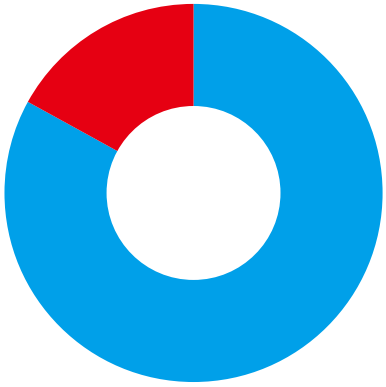

Research grant income from public sources and charities	1,960	83%
Research contract income from industry and commerce	410	17%

Government-Sponsored Research Fund (2016)

Unit: Million NTD (30 NTD ≈ 1 USD)

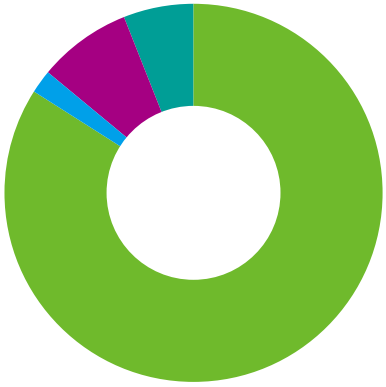

National Science Council	1,651	84%
Ministry of Economy	30	2%
Ministry of Education	159	8%
Others	120	6%

Non-Government Sponsored Research Fund (2016)

Unit: Million NTD (30 NTD ≈ 1 USD)

Non-Profit Organization	188	46%
Industry	195	47%
Overseas	27	7%

R & D Facts and Figures

Taiwan Patent Application and Registration (2008-2016)

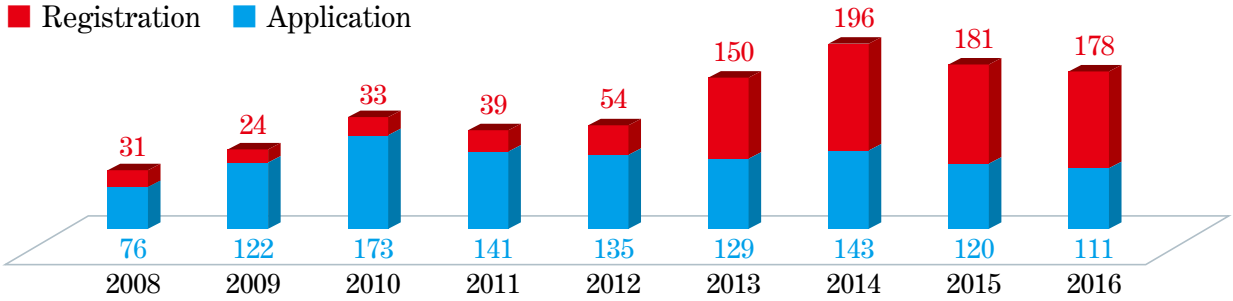

International Patent Application and Registration (2008-2016)

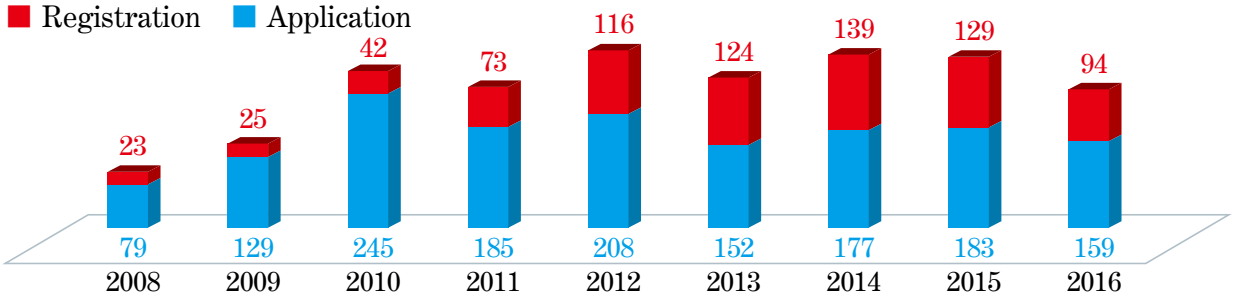

US Patent Application and Registration (2008-2016)

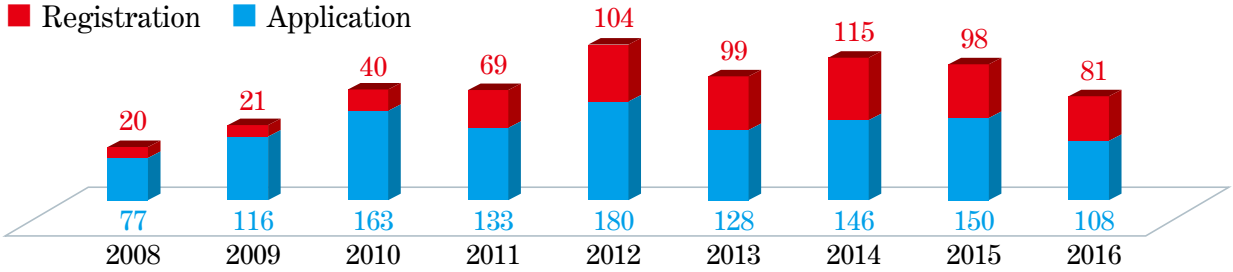

Technology Transfer Incomes (2008-2016)

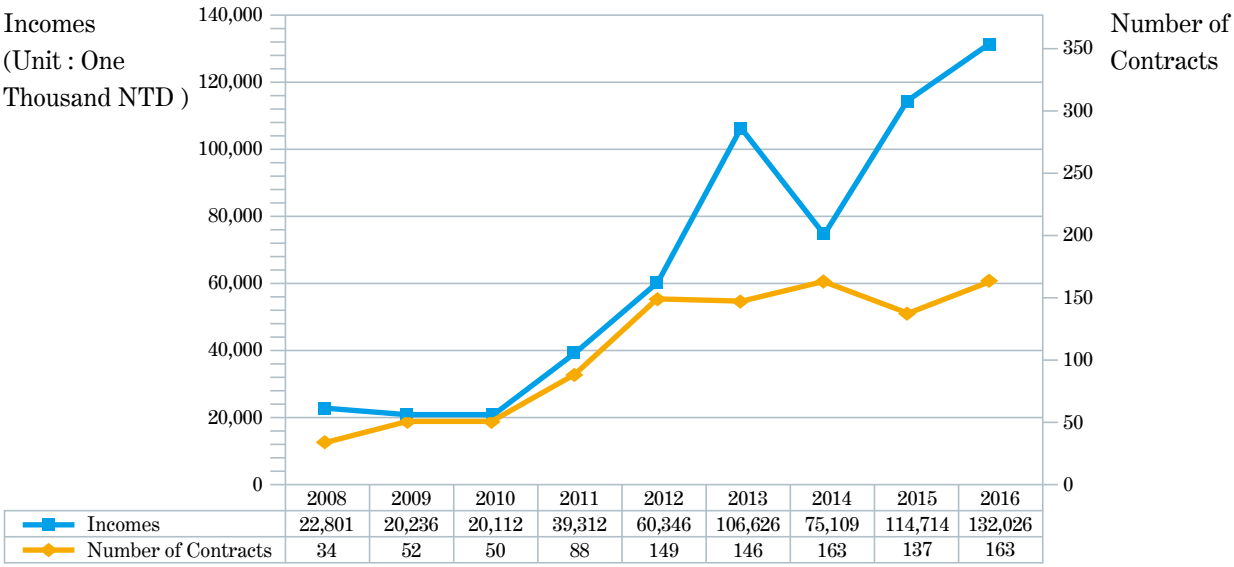

	2008	2009	2010	2011	2012	2013	2014	2015	2016
Incomes	22,801	20,236	20,112	39,312	60,346	106,626	75,109	114,714	132,026
Number of Contracts	34	52	50	88	149	146	163	137	163

Number of Paper (2007-2017)

Data sorce: Essential Science Indicators[SM]: year range:2007-2017

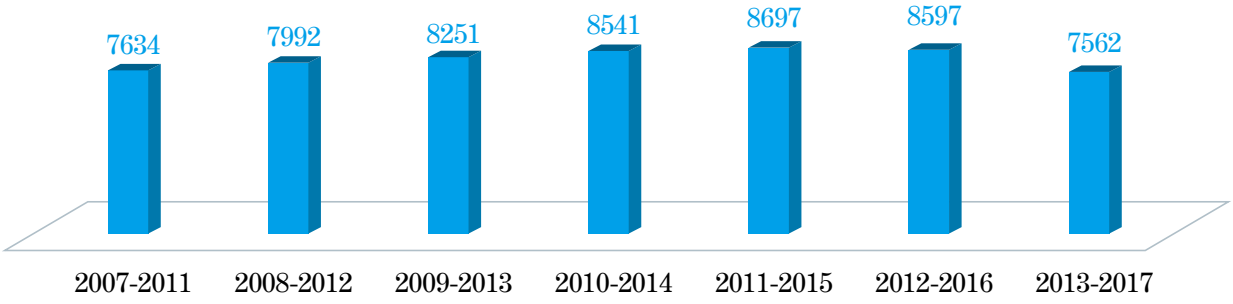

Citations Per Paper (2007-2017)

Data sorce: Essential Science Indicators[SM]: year range:2007-2017

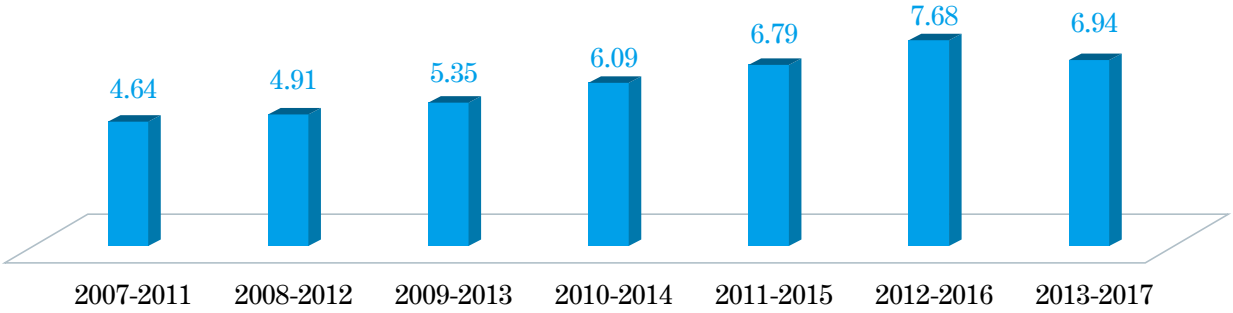

International Research Collaboration

(85 Countries / 1,421 Institutions / 50,283 Articles)

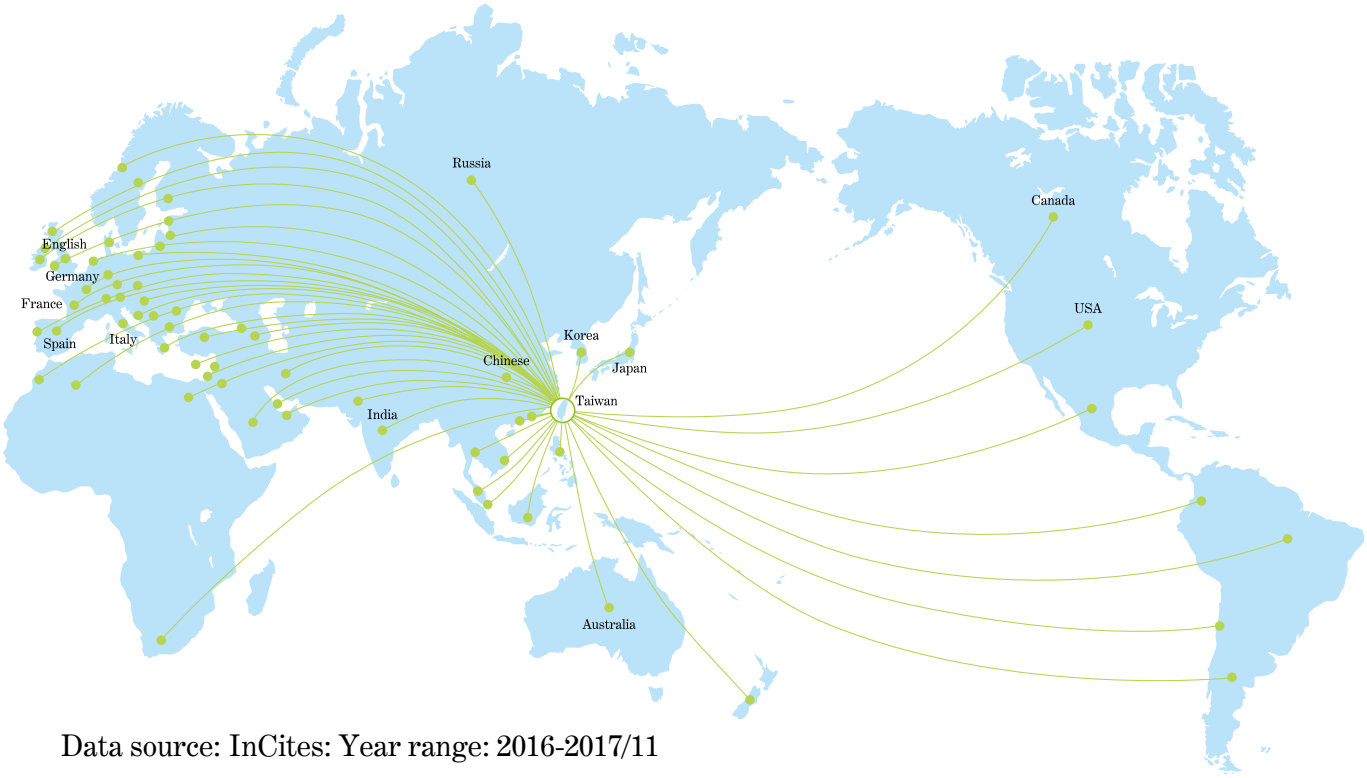

Data source: InCites: Year range: 2016-2017/11

Scientific Breakthroughs

Visible Light Copper Photoredox-catalyzed Aerobic Oxidative Coupling of Phenol and Terminal alkynes: Regioselctive Synthesis of Functionalized Ketones via C≡C Triple Bond Cleavage

Prof. Kuo Chu Hwang
Department of Chemistry

J. Am. Chem. Soc., 2017, 139(8), 2896–2899.

Direct oxidative coupling of phenols and terminal alkynes were achieved at room temperature by visible light-mediated copper-catalyzed photoredox process. This method allows regioselective synthesis of hydroxyl-functionalized aryl and alkyl ketones from simple phenols and phenylacetylene via C≡C triple bond cleavage. 47 examples were presented. From synthetic point view, this protocol offers an efficient synthetic route for preparation of pharmaceutical drugs, such as, pitofenone and fenofibrate.

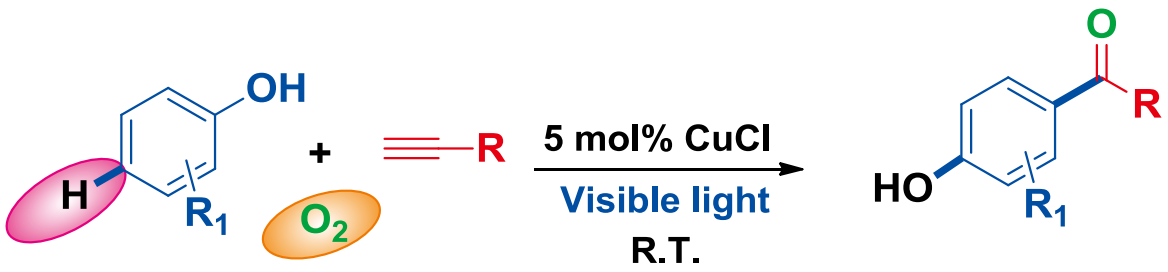

- Functionlized aryl/alkyl ketones
- oxidative C- functionlization of phenol
- Highly abundant phenols as starting materials
- C ≡ C triple bond cleavage

Authors

Arunachalam Sagadevan, Vaibhav Pramod Charpe, Ayyakkannu Ragupathi, and Kuo Chu Hwang*(黃國柱)
http://pubs.acs.org/doi/abs/10.1021/jacs.6b13113

Engineering Novel Targeted Boron-10 Enriched Theranostic Nanomedicine to Combat against Murine Brain Tumors via MR Imaging-Guided Boron Neutron Capture Therapy

Prof. Kuo Chu Hwang
Department of Chemistry

Adv. Mater. 2017, 29, 1700850

For the first time, an unprecedented ^{10}B-enriched boron nanoparticle-based theranostic nanomedicine (^{10}BSGRF NPs) were used to surpass the brain blood barrier (BBB), selectively target and effectively destruct murine brain tumors via magnetic resonance (MR) imaging-guided boron neutron capture therapy (BNCT).

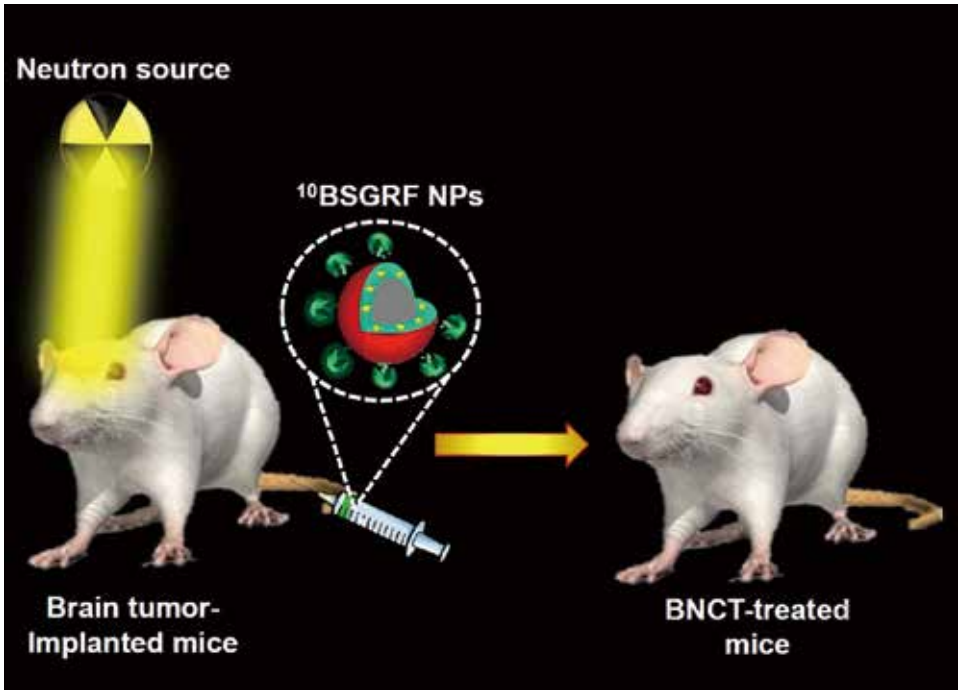

Authors

Naresh Kuthala, Raviraj Vankayala, Yi-Nan Li, Chi-Shiun Chiang, and Kuo Chu Hwang*(黃國柱)
http://onlinelibrary.wiley.com/doi/10.1002/adma.201700850/full

Handheld analyzer with on-chip molecularly-imprinted biosensors for electrical detection of propofol in plasma samples

Prof. Chien-Chong Hong
Department of Power Mechanical Engineering

Biosensors and Bioelectronics, 2016, 86, 623–629

- Molecularly imprinted polymer biosensors are and integrated with microfluidic biochips.
- Compared with the other methods, the proposed method is label-free, low-cost, and easy-to-use.
- Propofol detection with plastic biochip is demonstrated on a handheld electronic analyzer.

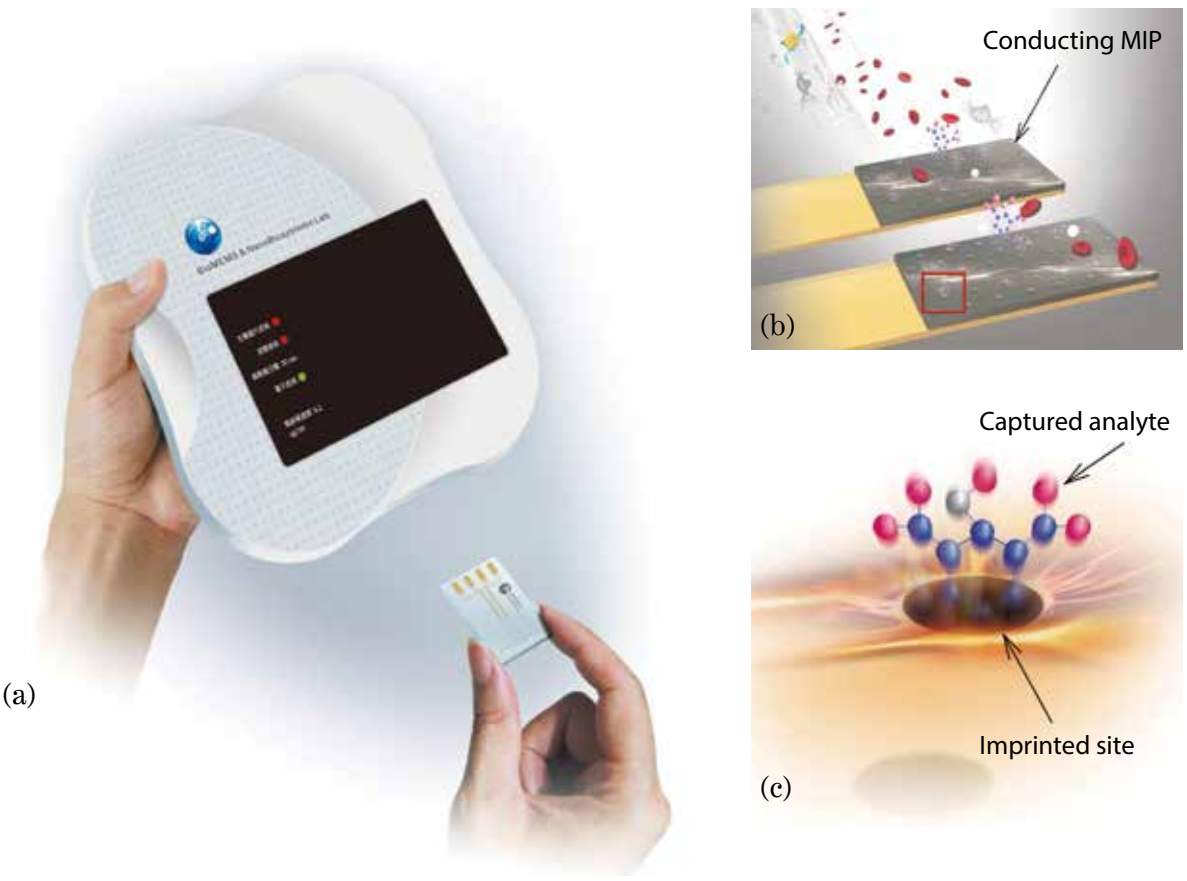

Scheme 1. Schematic of our developed propofol sensing system based on molecularly-imprinted biosensors. (a) handheld analyzer, (b) propofol capture and sensing on the molecularly imprinted biosensor, and (c) specific binding of propofol molecules in imprinted nanocavities.

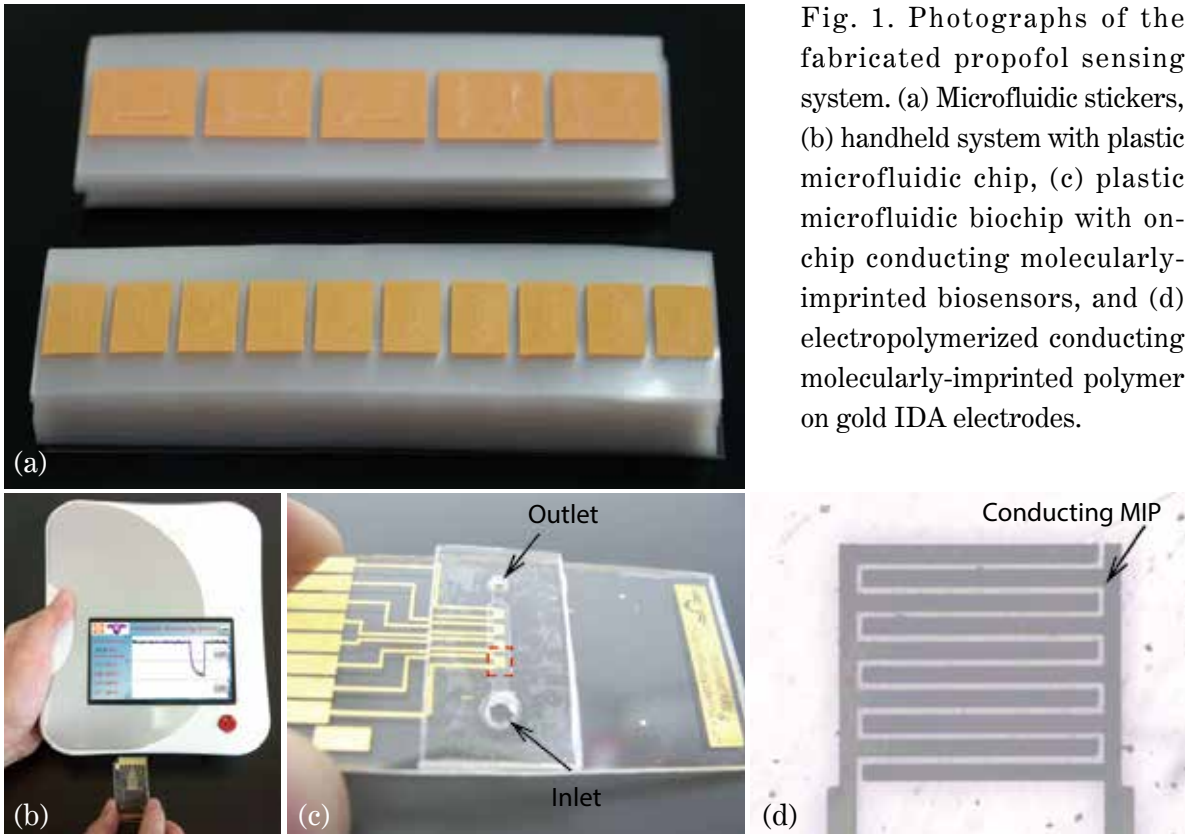

Fig. 1. Photographs of the fabricated propofol sensing system. (a) Microfluidic stickers, (b) handheld system with plastic microfluidic chip, (c) plastic microfluidic biochip with on-chip conducting molecularly-imprinted biosensors, and (d) electropolymerized conducting molecularly-imprinted polymer on gold IDA electrodes.

This paper proposes a novel handheld analyzer with disposable lab-on-a-chip technology for the electrical detection of the anesthetic propofol in human plasma samples for clinical diagnoses. The developed on-chip biosensors are based on the conduction of molecularly imprinted polymers (MIPs) that employ label-free electrical detection techniques. Propofol in total intravenous anesthesia is widely used with a target-controlled infusion system. At present, the methods employed for detecting blood propofol concentrations in hospitals comprise high-performance liquid chromatography and ion mobility spectrometry. These conventional instruments are bulky, expensive, and difficult to access. In this study, we developed a novel plastic microfluidic biochip with an on-chip anesthetic biosensor that was characterized for the rapid detection of propofol concentrations. The experimental results revealed that the response time of the developed propofol biosensors was 25 s. The specific binding of an MIP to a nonimprinted polymer (NIP) reached up to 560%. Moreover, the detection limit of the biosensors was 0.1 μg/mL, with a linear detection range of 0.1–30 μg/mL. The proposed disposable microfluidic biochip with an on-chip anesthetic biosensor using MIPs exhibited excellent performance in the separation and sensing of propofol molecules in the human plasma samples. Compared with large-scale conventional instruments, the developed microfluidic biochips with on-chip MIP biosensors present the advantages of a compact size, high selectivity, low cost, rapid response, and single-step detection.

Authors

Chien-Chong Hong (洪健中), Chih-Chung Lin, Chian-Lang Hong, Zi-Xiang Lin, Meng-Hua Chung, Pei-Wen Hsieh
https://doi.org/10.1016/j.bios.2016.07.032

Adipose-derived Stem Cell Sheets Functionalized by Hybrid Baculovirus for Prolonged GDNF Expression and Improved Nerve Regeneration

Prof. Yu-Chen Hu
Department of Chemical Engineering

Biomaterials Volume 140, September 2017, Pages 189-200

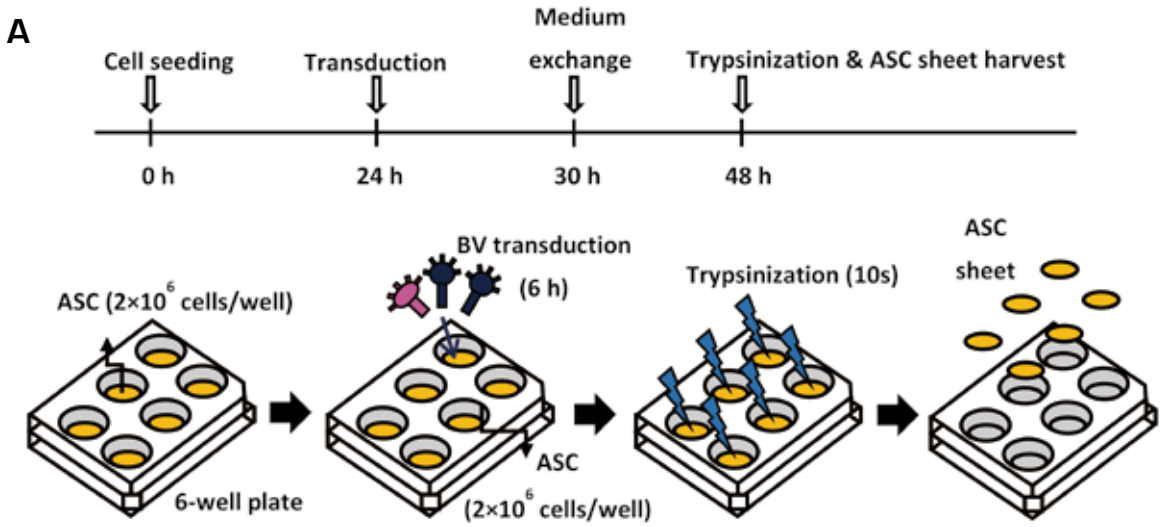

(A) Illustration of BV-transduced, GDNF-expressing ASCs sheets fabrication procedures.

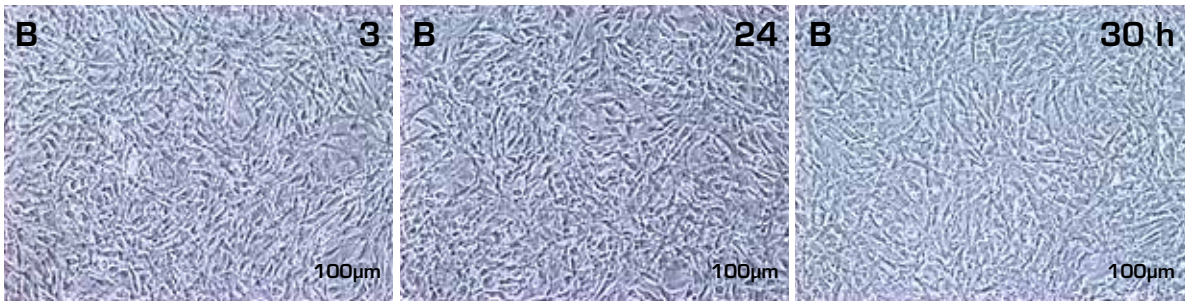

(B) Cell morphology at 3 h post-seeding.

(C) Cell morphology before transduction (24 h).

(D) Cell morphology after co-transduction with BacCre (MOI 100) and BacLEGW (MOI 100) at 30 h.

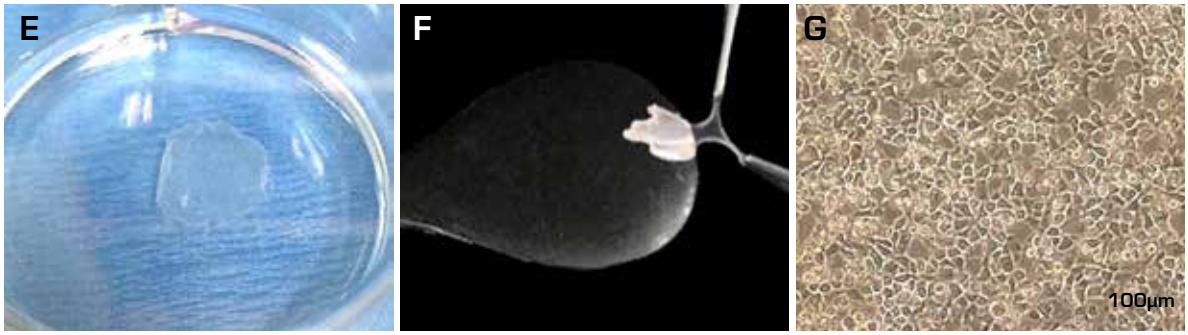

(E) Appearance of detached ASCs sheet after brief trypsinization.

(F) ASCs sheet that attached to the spatula.

(G) Cell morphology after the cell sheet re-attached to the 6-well plate.

Peripheral nerve regeneration requires coordinated functions of supporting cells (e.g. Schwann cells) and neurotrophic factors such as glial cell line-derived neurotrophic factor (GDNF), but nerve regeneration is usually far from complete. Here we constructed a Cre/loxP-based hybrid baculovirus (BV) vector which enabled intracellular formation of episomal DNA minicircle for effective transduction of rat adipose-derived stem cells (ASCs) and prolonged expression of functional GDNF capable of recruiting Schwann cells. The GDNF expression persisted for >20 days with the peak level (≈128 ng/ml) tremendously exceeding the picogram levels of GDNF secreted by neuroprogenitor cells. We further developed a facile method to fabricate and transduce cell sheets composed of undifferentiated ASCs in 2 days, without the need of thermo-responsive polymer commonly used for cell sheet fabrication. Implantation of the hybrid BV-engineered, GDNF-expressing ASCs sheets into sciatic nerve transection site in rats significantly improved the nerve repair, as judged from the enhanced functional recovery, nerve reinnervation, electrophysiological functionality, Schwann cells proliferation/infiltration, axon regeneration, myelination and angiogenesis. The hybrid BV is able to functionalize ASCs sheets by intracellular episomal DNA minicircle formation that circumvents undesired gene integration, and the ASCs sheets fabrication is rapid and simple. These data and features implicate the potentials of ASCs sheets functionalized by the hybrid BV for peripheral nerve regeneration.

Authors

Mu-Nung Hsu, Han-Tsung Liao, Kuei-Chang Li, Hwei-Hsien Chen, Tzu-Chen Yen, Pavel Makarevich, Yelena Parfyonova, Yu-Chen Hu (胡育誠)

http://www.sciencedirect.com/science/article/pii/S0142961217303101?via%3Dihub

Active Tumor Permeation and Uptake of Surface Charge-Switchable Theranostic Nanoparticles for Imaging-Guided Photothermal/Chemo Combinatorial Therapy

Prof. Hsin-Cheng Chiu
Department of Biomedical Engineering and Environmental Sciences

Theranostics, 6(3), 302-317 (2017)

Although the great advance in nanomedicine in the last two decades, the challenges in therapeutics delivery for cancer treatment still remain mostly owing to the drawbacks in short blood circulation time, low drug bioavailability, and poor tumor penetration/uptake. The surface modification of the drug carriers with poly(ethylene glycol) (PEG) and zwitterionic materials can efficiently increase drug residence in blood circulation and thus tumor accumulation. However, such modifications could impede the uptake of nanocarriers by cancer cells. Although it has shown that positively surface-charged nanoparticles exhibited promoted uptake by cancer cells via electrostatic attractions, their application in drug delivery is limited by rapid body elimination, tissue toxicity and reduced tumor penetration. Therefore, it is in great demand to develop smart drug delivery systems which can prevent or reduce non-specific protein adsorption during blood circulation, yet still be actively transformed into a more cell-interactive structure once localized and accumulated in tumor tissues.

To substantially promote tumor uptake and penetration of therapeutics, a nanovehicle system comprising poly(lactic-co-glycolic acid) (PLGA) as the hydrophobic cores coated with pH-responsive N-acetyl histidine modified D-α-tocopheryl polyethylene glycol succinate (NAcHis-TPGS), NHTPNs, was developed in this work. The nanocarriers with switchable surface charges in response to tumor extracellular acidity (pHe) were capable of selectively co-delivering indocyanine green (ICG), a photothermal agent, and doxorubicin (DOX), a chemotherapy drug, to tumor sites. The in vitro cellular uptake of ICG/DOX-loaded nanoparticles by cancer cells and macrophages was significantly promoted in weak acidic environments due to the increased protonation of the NAcHis moieties. The results of the in vivo and ex vivo biodistribution studies demonstrated that upon intravenous injection the theranostic nanoparticles were appreciably accumulated in TRAMP-C1 solid tumor of tumor-bearing mice. The immunohistochemical examination of tumor sections confirmed the active permeation of the nanoparticles into deep tumor hypoxia regions due to their small size, pHe-induced near neutral surface, and the additional hitchhiking transport via tumor-associated macrophages. The prominent imaging-guided photothermal therapy of ICG/DOX-loaded nanoparticles after tumor

accumulation induced extensive tumor tissue/vessel ablation, which further promoted their extravasation with the DOX tumor permeation, thus effectively suppressing tumor growth.

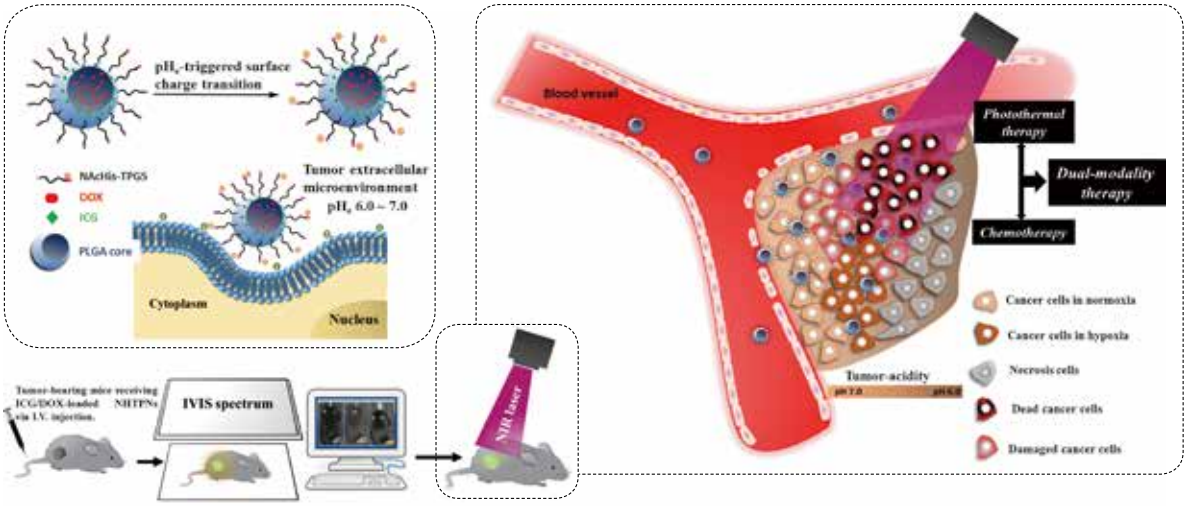

Figure 1. Illustration of active tumor penetration and uptake of dual therapeutics-loaded nanoparticles with pHe-triggered surface charge transition for the imaging-guided photothermal/chemo combinatorial therapy.

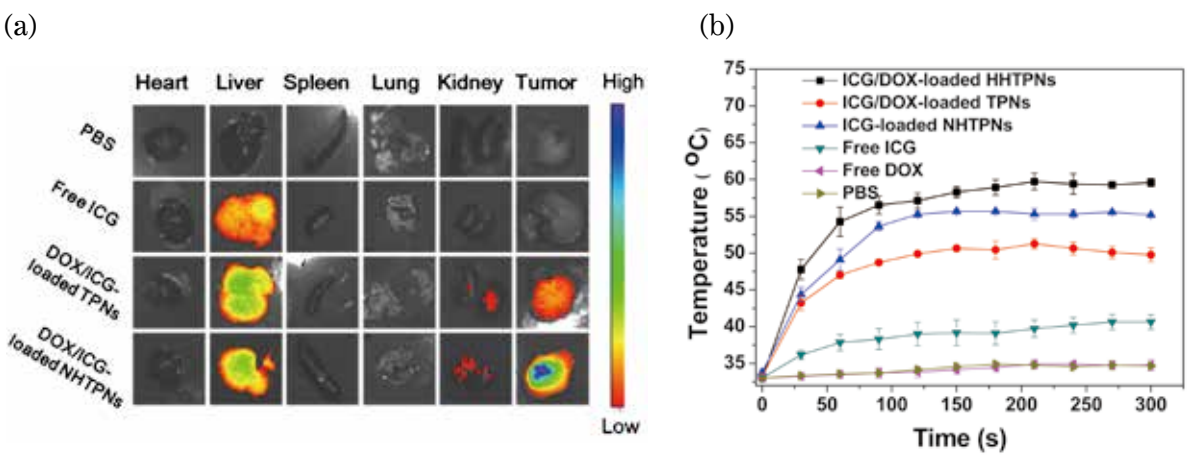

Figure 2. (a) NIR fluorescence images of the isolated major organs and tumors. The NHTPNs were appreciably accumulated within the lesion region. (b) Tumor growth profiles of the mice bearing TRAMP-C1 tumor intravenously injected with various formulations, demonstrating that the dual-modality therapy delivered by NHTPNs exhibited the prominent antitumor efficacy.

Authors

Chia-Chian Hung, Wen-Chia Huang, Yi-Wen Lin, Ting-Wei Yu, Hsin-Hung Chen, Sung-Chyr Lin, Wen-Hsuan Chiang, Hsin-Cheng Chiu (邱信程)
http://www.thno.org/v06p0302

Synthesis of Nonepitaxial Multilayer Silicene Assisted by Ion Implantation

Prof. Jenq-Horng Liang
Institute of Nuclear Engineering and Science

Nanoscale, 2016, 8, 9488-9492

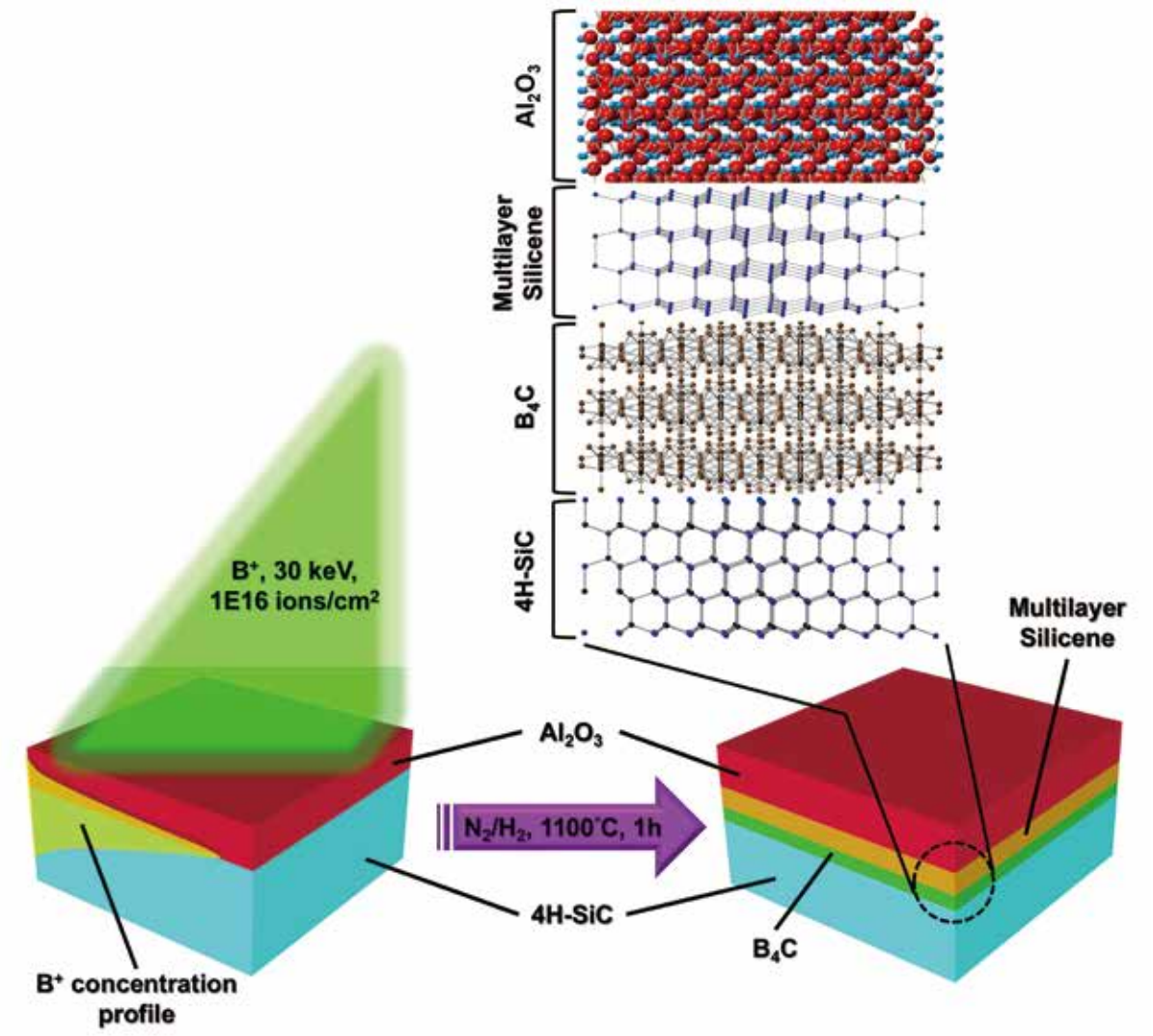

The illustration of the implantation-assisted process and the atomic model of layer structure comprising Al_2O_3, multilayer silicene, B_4C, and 4H-SiC substrate.

Nonepitaxial multilayer silicene with lonsdaleite structure has been first synthesized from 4H-SiC substrate using an implantation-assisted process in this investigation. The sp^3-like bonding signal from lonsdaleite Si was first fitted in the Si 2p XPS spectrum. The multilayer silicene can be directly observed and the derived interplanar distances are nearly consistent with the theoretical values.

The results of material analysis verify that the carbon at the surface of SiC has preferentially reacted with the boron ions from implantation to form B_4C during annealing, simultaneously; the silicon atoms would be squeezed out of the surface to rearrange themselves into multilayer silicene. The priority of occurrence between two chemical reactions depends on the ΔG values of them. In this case, the ΔG of B_4C formation is much more negative than that of silicon boride (SiBn) formation under the particular condition. Thus the former is a spontaneous reaction and the latter is not, resulting in the silicon condensation on the surface. Most importantly, the critical factors for the formation of multilayer silicene, rather than that of diamond-structured silicon, need to be clarified. We suppose that the silicon atoms, which are initially condensed onto the surface, tend to crystallize into the cubic diamond structure under annealing. Then, the high stress resulting from the lattice mismatch between Si and B_4C constrains the lattice constant of Si; meanwhile, the thermal energy promotes the cubic diamond Si, which is metastable at 1100° C, transforming into hexagonal lonsdaleite Si (multilayer silicene). This variation course of crystal structure is the so-called stress-induced phase transformation.

In conclusion, we successfully modify the plasma-assisted process by replacing the plasma with ion implantation to synthesize the nonepitaxial multilayer silicene for the first time. The yield of this simple process is stable and reproducible. The results of material analysis are totally in agreement with the computational results. The synthesis mechanism has been clearly interpreted by thermodynamics and phase transformation. The multilayer silicene possesses significant potential to be a material applied to electronic devices, and the synthesis method in this study could be further developed. In the future, the multilayer silicene FET devices could be fabricated combining this synthesis method. It is worth noting that the Al_2O_3 capping layer may not only plays the role of protective layer but also the gate dielectrics.

Authors

Hsu-Sheng Tsai, Ching-Hung Hsiao, Chia-Wei Chen, Hao Ouyang, Jenq-Horng Liang (梁正宏)
http://pubs.rsc.org/-/content/articlehtml/2016/nr/c6nr02274j

Expression of Neuroendocrine Factor VGF in Lung Cancer Cells Confers Resistance to EGFR Kinase Inhibitors and Triggers Epithelial-to-Mesenchymal Transition

Prof. Yu-Ting Chou
Institute of Biotechnology

Cancer Research 77(11): 3013-3026 (2017)

Lung cancer is the leading cause of cancer death in the world and ranks first among cancer mortality in Taiwan. Cancer metastasis and drug resistance are main causes of lung cancer-related death. Recently, we reported that lung cancer cell populations generate cancer metastasis and drug resistance by switching differential lineage programs, and thus generating cancer plasticity to cope with drug selection pressures and promote invasive capabilities.

Identification of effective biomarkers and therapeutic targets has improved precedence in drug discovery and personalized therapy. Lung cancer patients harboring EGFR in-frame deletions in exon 19 or the exon 21 mutation L858R benefit from treatment with EGFR tyrosine kinase inhibitors (TKIs), supporting the notion that lung cancer is under EGFR oncogene addiction. Nonetheless, the development of EGFR-TKI drug resistance invariably occurs. Moreover, metastases are commonly observed in patients with EGFR-mutated lung adenocarcinoma, whereas the molecular mechanism is unknown. Phenotypic alteration in epithelial-to-mesenchymal transition (EMT) has been linked to the resistance of EGFR-TKI in lung cancer. However, the mechanism underlying this resistance remains unclear. We discovered that cancer plasticity induced by a neuroendocrine factor termed VGF endows cancer cells with TKI resistance, EMT, and invasiveness. We developed a serial of methods to detect VGF expression in lung tumors and serum. Correlation analysis revealed a significant association of VGF expression with advanced tumor grade and poor survival in patients with lung adenocarcinoma, indicating VGF as a novel prognostic biomarker for lung cancer progression. VGF silencing inhibited lung cancer cell growth and resensitized EGFR-mutated lung adenocarcinoma cells to TKI. In a mouse xenograft model of lung adenocarcinoma, suppressing VGF expression was sufficient to attenuate tumor growth. Overall, our findings show how VGF can trigger cancer plasticity towards EMT and confer TKI resistance, suggesting its potential utility as a novel biomarker and therapeutic target in lung adenocarcinoma.

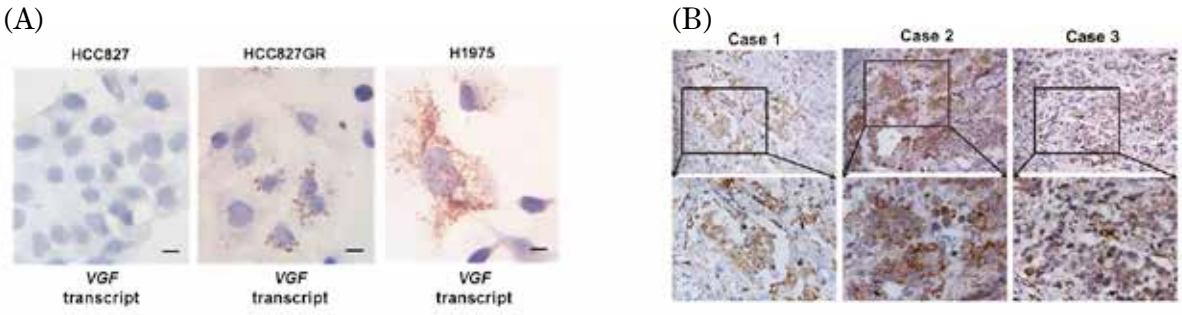

Figure 1. *VGF* expression in neuroendocrine carcinoma and EGFR-TKI resistant tumors. (A) RNA *in situ* analysis of *VGF* mRNA expression in HCC827 (TKI sensitive, left), HCC827GR (TKI resistant, middle), and H1975 (TKI resistant, right) lung cancer cells. (B) Immunohistochemical analysis of VGF expression in three cases of lung cancer. Case 1: treatment-naïve neuroendocrine carcinoma; case 2 and case 3: acquired EGFR-TKI resistant lung adenocarcinomas harboring EGFR Del19/T790M mutations.

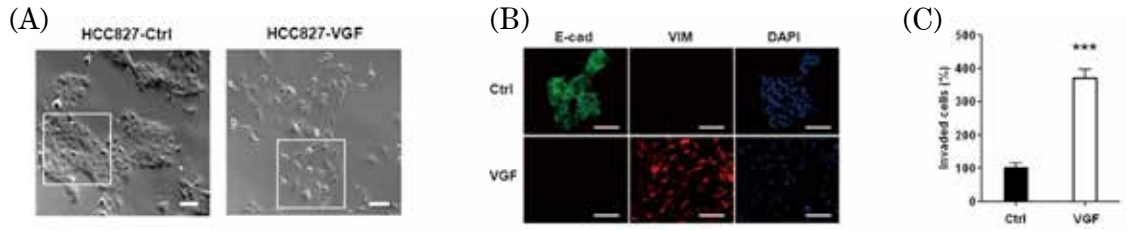

Figure 2. VGF induces EMT and TKI resistance. (A) Representative phase-contrast images of HCC827 cells infected with the lentiviral vector encoding cDNA of *VGF* (HCC827-VGF) or empty control vector (HCC827-Ctrl). (B) Immunofluorescence of E-cadherin (E-cad) and Vimentin (VIM) expression in HCC827-Ctrl (Ctrl) and HCC827-VGF (VGF) cells. Nuclei were stained in blue with DAPI. (C) Transwell matrigel invasion analysis of HCC827-Ctrl and HCC827-VGF cells.

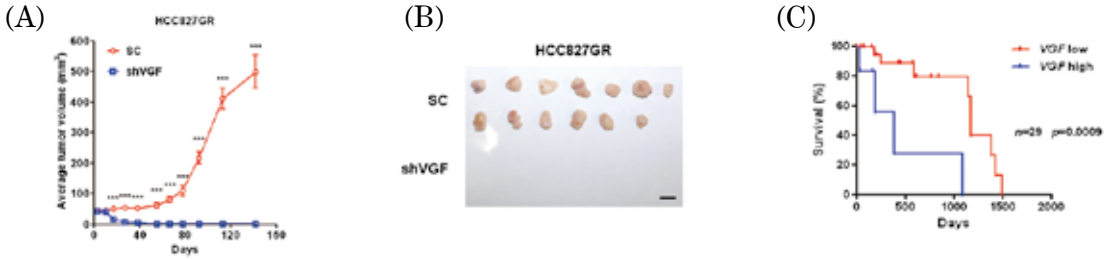

Figure 3. VGF functions as the therapeutic target and prognostic biomarker in lung cancer. (A) Xenograft assay for assessing the effect of VGF silencing on tumor growth. HCC827GR cells were infected with lentiviral vector encoding shVGF (shVGF) or scrambled control (SC) and further injected subcutaneously into nude mice. Tumor volume was monitored over time as indicated (left). The representative photographs illustrate tumor growth 140 days after injection (right). (B) Kaplan–Meier analysis to assess the correlation of *VGF* expression with the overall survival of EGFR-mutated lung adenocarcinoma from the TCGA (LUAD) database.

Authors

Wen Hwang, Yu-Fan Chiu, Ming-Han Kuo, Richard Lee, An-Chun Lee, Chia-Cherng Yu, Junn-Liang Chang, Wen-Chien Huang, Shih-Hsin Hsiao, Sey-En Lin, Yu-Ting Chou (周裕斑)
http://cancerres.aacrjournals.org/content/77/11/3013.long

DynOmics: dynamics of structural proteome and beyond

Prof. Lee-Wei Yang
Institute of Bioinformatics and Structural Biology

Nucleic Acids Research, 45, W374–W380 (2017); 44, D415-D422 (2016)

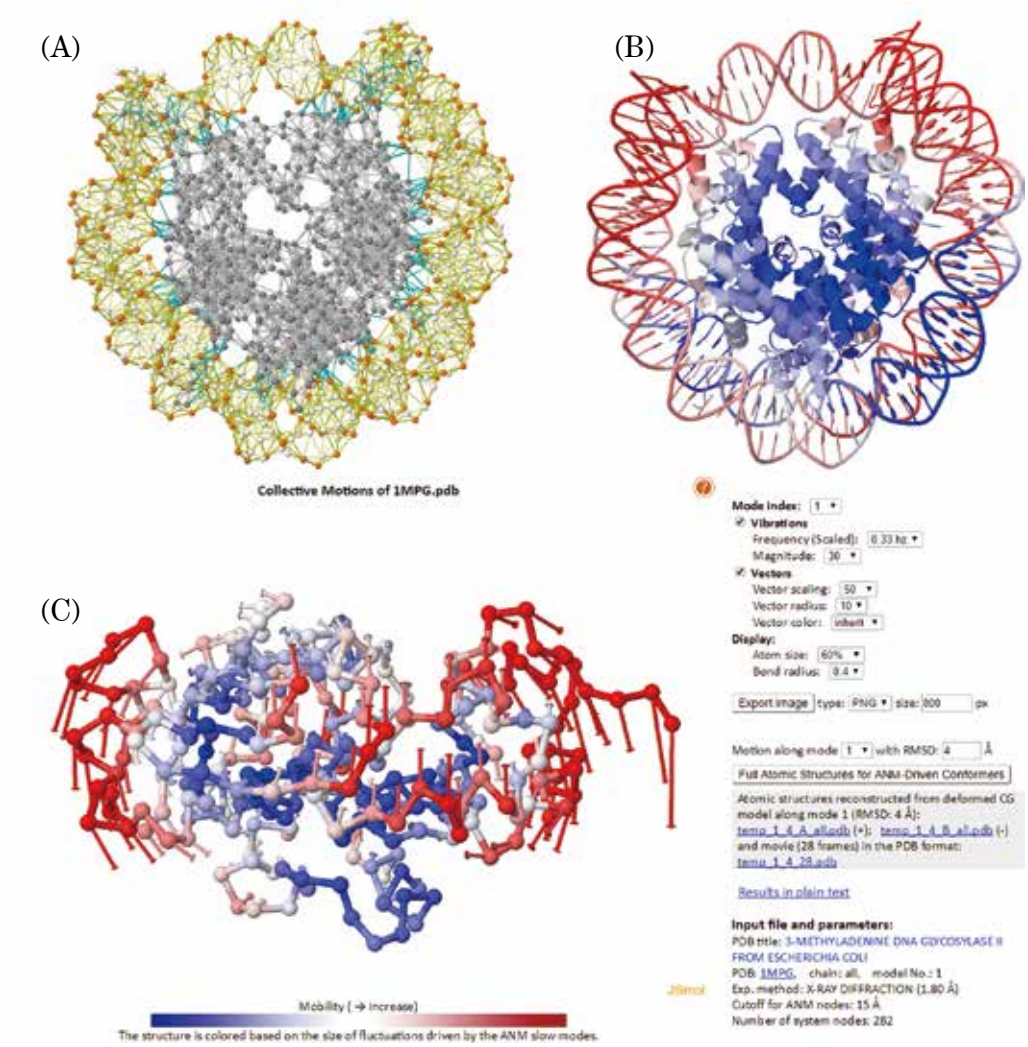

GNM representation of biomolecular structures and color-coded ribbon diagrams (reproduced from ref [2]) used in the *i*GNM DB (http://dyn.life.nthu.edu.tw/gnmdb/). A coarse-grained (CG-) representation (A), consisting of nodes at the positions of the C^{α}-atoms (*gray*) in proteins, and at the P (*orange*), C4‘- and C2-atoms (*white*) in DNA/RNA, for the nucleosome core particle (PDB id: 1KX4). Panel (B) is the ribbon diagram for its all-atom model. (C) A snapshot from “Molecular Motions” (reproduced from ref [1]), generated by ENM 1.0 (http://dyn.life.nthu.edu.tw/oENM/). A snapshot from the animation generated for 3-methyladenine DNA glycosylase (PDB: 1MPG) slowest mode (*mode 1*) is shown. The protein is in CG representation, color-coded based on the size of motions (*red*: most mobile, *blue*: most rigid) calculated from anisotropic network model (ANM).

DynOmics is a portal that integrates rapidly growing structural proteomics data and evaluates the functional dynamics of structurally resolved biomolecules, in a consistent theoretical framework at their physiological environment. Central to the portal lies the newly designed calculation engine, ENM 1.0 (http://dyn.life.nthu.edu.tw/oENM/), which permits users to efficiently generate information on collective dynamics of any structure in a PDB format, user-uploaded or database-retrievable (from *i*GNM2.0, http://dyn.life.nthu.edu.tw/gnmdb/). ENM 1.0 integrates two widely used coarse-grained elastic network models (ENMs) — the Gaussian Network Model (GNM) and the Anisotropic Network Model (ANM), reformulated to consider the molecular "environment". It allows users to predict potentially functional sites according to solvent exposed and spatially clustered mechanical hinges, assess key sites in allosteric communication, and cull dynamically possible protein–protein and protein–DNA interaction poses, in addition to rendering ANM-deformed conformers reconstructed at atomistic resolution. The 'environment' is considered and implemented with high flexibility, from substrate or ligands bound to a protein, to lipid bilayer and crystal contacts, or surrounding subunits in multimeric structures or assembly. User-friendly interactive features permit users to easily visualize and compare the query systems in the presence or absence of the "environment". ENM 1.0 is readily accessible at http://dyn.life.nthu.edu.tw/oENM/, empowered by NTHU.

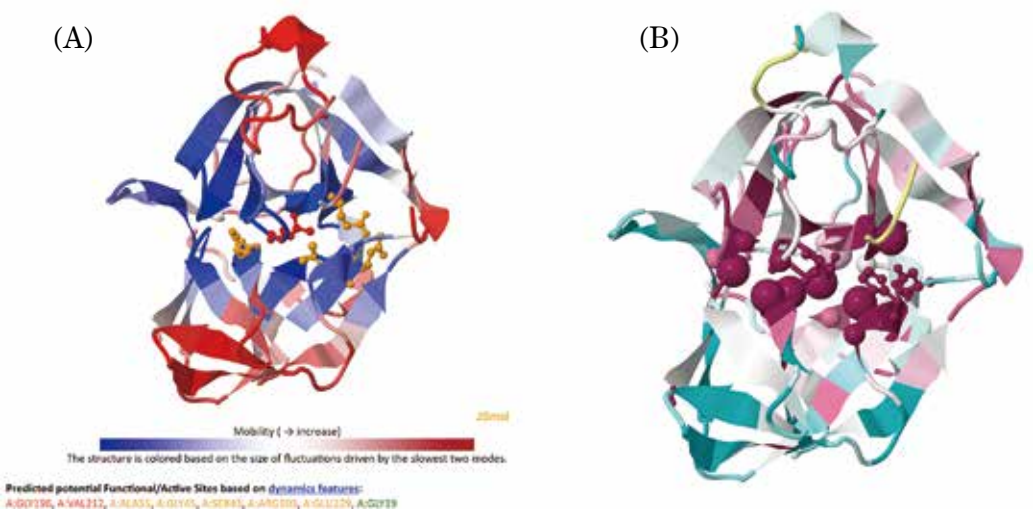

Characterization of potentially functional sites by DynOmics. (reproduced from ref [1]) (A) PFSs predicted by COMPACT implemented in *ENM 1.0* (http://dyn.life.nthu.edu.tw/oENM/), illustrated for alpha-lytic protease (PDB: 2LPR), shown in *ball and stick* (snapshot from the web interface). (B) The same enzyme, color-coded by sequence conservation (*dark magenta*: most conserved; *cyan*: most variable). Predicted hinges and PFSs are shown in van der Waals spheres, catalytic sites as *ball-and-stick*.

Authors

Hongchun Li, Yuan-Yu Chang, Ji Young Lee, Ivet Bahar and Lee-Wei Yang (楊立威)

[1] DynOmics: https://academic.oup.com/nar/article/45/W1/W374/3791214/
[2] iGNM 2.0: https://academic.oup.com/nar/article-lookup/doi/10.1093/nar/gkv1236

Making an Impact on Technology

Large Cross-Phase Modulations at the Few-Photon Level

Prof. Ite A. Yu
Department of Physics and Frontier Research Center on Fundamental and Applied Sciences of Matters

Physical Review Letters 117, 203601 (2016)

Quantum information is the wave function in quantum mechanics. Wave functions can neither be duplicated nor be amplified. Preservation or protection of wave functions is an important issue in quantum information science. One can employ electrons, atoms, molecules, or larger particles to carry wave functions. However, wave functions of these particles are fragile in the presence of stray fields from the environment or due to collisions among each other. It is difficult to preserve the fidelity of the information carried by these particles during the transmission. On the other hand, photons are ideal carriers of information as they possess ultimate propagation speed, hardly interact with the environment, and never collide with each other. Light pulses with rather many photons are classical electromagnetic waves, but those with few or single photons exhibit quantum nature governed by quantum mechanics (i.e. quantum optics). We have seen that classical light is widely utilized in the telecommunication technology. Similarly, we can foresee photons will be employed to carry quantum information among quantum networks and in long-distance quantum communication because of their excellent fidelity for carried wave functions.

Slow light and stopped light arising from the effect of electromagnetically induced transparency (EIT) make quantum information manipulation with photons feasible. Slow light greatly enhances the interaction time between light and matter, and achieves significant efficiencies of nonlinear optical processes at single-photon level. Stopped light provides the method of coherent transfer of wave functions between photons and atoms and has the great potential in quantum memory.

A qubit (quantum bit) is essentially a single photon. It is a rather challenging and difficult task to make a single photon interact with another, i.e. qubit-qubit operation. In this work, we proposed and experimentally demonstrated a novel scheme of cross-phase modulation (XPM) utilizing slow light in a double-EIT system (see Figure 1). XPM refers to the process that the phase of a light pulse is modulated by another. The photon-photon interaction mediated by the double-EIT system can be controlled by varying the relative phase of applied light fields. This phase-dependent XPM scheme can achieve large phase modulations at single-photon level without requiring cavities or tightly focusing laser beams. We observed a phase shift of about π with two light pulses, both consisting of 8 photons. The experiment was carried out in laser-cooled ^{87}Rb atoms.
The paper of our work is selected as Editors'

Suggestion, and also reported by a Viewpoint in *Physics*, entitled "Optical Quantum Logic at the Ultimate Limit". As quoted from the article, *"Finally, Ite Yu from the National Tsing Hua University, Taiwan, and colleagues made two pulses—each containing, on average, eight photons—propagate slowly and simultaneously through a cold-atom cloud in which two EIT configurations overlapped. ..... The shift is equivalent to 26 per photon, with the prospect of further improvement."*

Our scheme provides a simple route to generate strong interactions between photons and may have potential applications in all-optical quantum signal processing.

This work was done under a collaboration project (Science Vanguard Research Program of MOST) with I. A. Yu as the project leader and Y.-C. Chen and Y.-F. Chen as the subproject leaders.

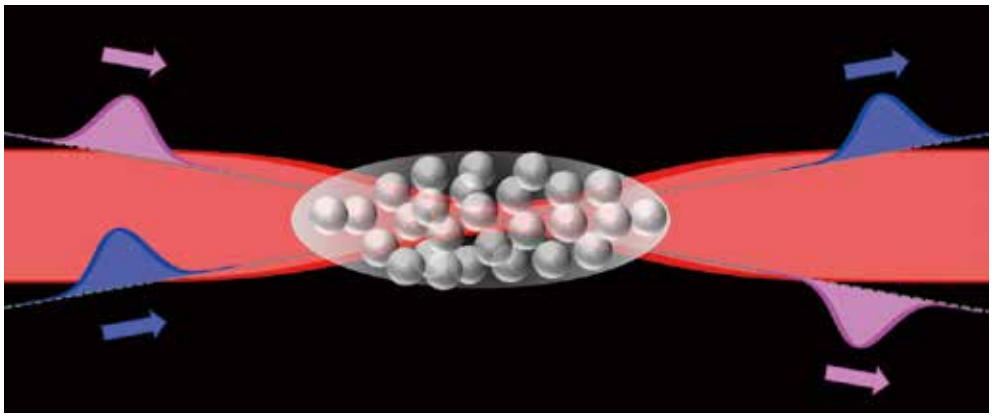

Figure 1: Two light pulses (blue and purple) and two continuous-wave laser fields (red) propagate through a cloud of cold atoms, forming the scheme of cross-phase modulation based on the double-EIT system. The phase of purple pulse was shifted by 180 degrees due to the presence of blue pulse. Both light pulses consisted of only 8 photons and had the actual wavelength of 780 nm.

Authors

Zi-Yu Liu, Yi-Hsin Chen, Yen-Chun Chen, Hsiang-Yu Lo, Pin-Ju Tsai, Ite A. Yu (余怡德), Ying-Cheng Chen and Yong-Fan Chen
https://journals.aps.org/prl/abstract/10.1103/PhysRevLett.117.203601

A Generalized Quasi-MMSE Controller for Run-to-Run Dynamic Models

Prof. Sheng-Tsaing Tseng
Institute of Statistics

Technometrics, 59(3), 381-390, 2017

Run-to-run (RTR) process control techniques are frequently used in semiconductor manufacturing operations. RTR techniques have been successfully applied to several semiconductor manufacturing processes such as photolithography process, chemical mechanical polishing (CMP) process, reactive ion etching (RIE), etc. The key idea of RTR control is to adjust the process output to its desired target. Process dynamics and process disturbance are very common in a complex semiconductor manufacturing process. Assuming that x_{t-1} and Y_t denote the input recipe and output response at time t, respectively, the input-output relationship of an SISO process is postulated in terms of the following dynamic model:

$$\left(1-\delta_1 \mathrm{B}-\delta_2 \mathrm{B}^2-\ldots-\delta_r \mathrm{B}^r\right) Y_t = \alpha+\left(\gamma_0-\gamma_1 \mathrm{B}-\gamma_2 \mathrm{B}^2-\ldots-\gamma_s \mathrm{B}^s\right) x_{t-b}+\eta_t, \qquad (1)$$

where B is a backshift operator and α is the intercept parameter of the process; $\{\delta_i\}_{i=1}^{r}$ and $\{\gamma_j\}_{j=0}^{s}$ are the carryover effects for the output responses and input recipes, respectively. Furthermore, we assume that η_t (process disturbance) follows an ARIMA (p, d, q) series. In other words, $(1-\sum_{i=1}^{p}\phi_i \mathrm{B}^i)(1-\mathrm{B})^d \eta_t = (1-\sum_{j=1}^{q}\theta_j \mathrm{B}^j)\varepsilon_t$ where d is a nonnegative integer; $\{\phi_i\}_{i=1}^{p}$ and $\{\theta_j\}_{j=1}^{q}$ are the autoregressive and moving average parameters, respectively. Let τ denote the desired target of process outputs. In this study, we proposed a generalized quasi-MMSE controller as follows:

$$x_t = x_{t-1} - \frac{\omega+\hat{\delta}_1+\sum_{j=2}^{r}\left(\hat{\delta}_j-\hat{\delta}_{j-1}\right)\mathrm{B}^{j-1}-\hat{\delta}_r \mathrm{B}^r+\hat{\phi}_1(1-\mathrm{B})(1-\sum_{i=1}^{r}\hat{\delta}_i \mathrm{B}^i)}{\left(\hat{\gamma}_0-\hat{\gamma}_1 \mathrm{B}-\ldots-\hat{\gamma}_s \mathrm{B}^s\right)(1-\hat{\phi}_1 \mathrm{B})}\left(Y_t-\tau\right). \qquad (2)$$

Let **Q** be a square matrix of order (r+s+3) as follows:

$$\mathbf{Q} = \left(\begin{array}{ccc|c|ccc} c_1 & \cdots & c_{r+1} & c_{r+2} & c_{r+3} & \cdots & c_{r+s+2} & c_{r+s+3} \\ \hline 1 & \cdots & 0 & 0 & 0 & \cdots & 0 & 0 \\ \vdots & \ddots & 0 & \vdots & \vdots & \ddots & & \vdots \\ 0 & \cdots & 1 & 0 & 0 & \cdots & 0 & 0 \\ \hline a_1 & \cdots & a_{r+1} & a_{r+2} & a_{r+3} & \cdots & a_{r+s+2} & a_{r+s+3} \\ \hline 0 & \cdots & 0 & 0 & 1 & \cdots & 0 & 0 \\ \vdots & \ddots & & \vdots & \vdots & \ddots & \vdots & \vdots \\ 0 & \cdots & 0 & 0 & 0 & \cdots & 1 & 0 \end{array}\right),$$

where $\{a_i\}$ and $\{c_i\}$ are suitable functions of $\{\hat{\delta}_i\}$, $\{\hat{\gamma}_i\}$ and $\{\hat{\phi}_1\}$.

Main Result of this study:

If $d \leq 1$ and the maximum absolute values of the eigenvalues of **Q** *is less than 1, then* $\lim_{t\to\infty} E(Y_t)=\tau$, and $\lim_{t\to\infty} \mathrm{Var}(Y_t)< \infty$. *Furthermore, the asymptotic distribution of the controlled output follows a stationary* ARMA($r+s+p+3, s+q+2-d$) *process.*

An example of chemical mechanical polishing (CMP) process is used to illustrate the performance of the proposed method. Let Y_t and x_{t-1} denote the removal rate and the platen speed (which is normalized to the range of (-3, 3)) of CMP process for run t, respectively. Assume that τ =1800(Angstrom). This study adopts the following dynamic model as the plant I-O model:

$$Y_t=0.53Y_{t-1}+0.3Y_{t-2}+633+96.3x_{t-1}+32.1x_{t-2}+23.5x_{t-3}+\eta_t$$

where η_t is an ARIMA(1,1,1) series with parameters, ϕ_1 =-0.1, θ_1=-0.44, and $\varepsilon_t \overset{iid}{\sim} N(0,40^2)$, t=1,....
Four models and their estimates of unknown parameters are:

(1) $(\hat{\delta}_1, \hat{\delta}_2, \hat{\gamma}_0, \hat{\gamma}_1, \hat{\gamma}_2, \hat{\phi}_1) = (0.503, 0.292, 98.382, -28.868, -28.874, -0.149)$;

(2) $(\hat{\delta}_1, \hat{\delta}_2, \hat{\gamma}_0, \hat{\gamma}_1, \hat{\phi}_1) = (0.427, 0.408, 91.892, -31.846, 0.149)$;

(3) $(\hat{\delta}_1, \hat{\gamma}_0, \hat{\gamma}_1, \hat{\gamma}_2, \hat{\phi}_1) = (0.769, 94.720, -6.677, -28.181, -0.679)$; and

(4) $(\hat{\delta}_1, \hat{\gamma}_0, \hat{\gamma}_1, \hat{\phi}_1) = (0.821, 81.095, 9.120, -0.678)$.

All of the process outputs converge to the desired target, but the convergence rates to the desired target under (*r, s*)=(*2, 2*) and (*r, s*)=(1, 2) are faster than those in the other two cases. The outputs controlled by four qMMSE controllers (with their individual optimal discount factors) are shown in Figure 1. Furthermore, the results demonstrate that the model mis-specification effects on the TMSE are not negligible (the proportions of TMSE will increase up to 40.3% and 44.0%, respectively), when the process I-O model was wrongly mis-identified as (*r, s*)=(*2, 1*) and (*r, s*) = (1, 1). This means that the effects of mis-identification of the process I-O model on the process total mean square error (TMSE) is not negligible for implementing a dynamic RTR process control.

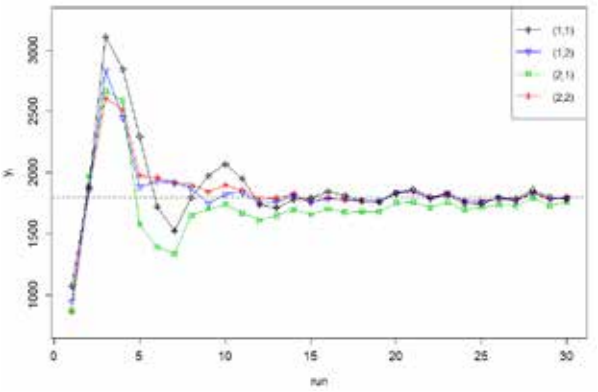

Figure 1: Controlled outputs by the qMMSE controllers with different orders.

Authors

Sheng-Tsaing Tseng (曾勝滄) and Pei-Yu Chen
http://amstat.tandfonline.com/doi/full/10.1080/00401706.2016.1228547

A Heat-Resistant $NiCo_{0.6}Fe_{0.2}Cr_{1.5}SiAlTi_{0.2}$ Overlay Coating for High-Temperature Applications

Prof. Jien-Wei Yeh
Department of Materials Science and Engineering

Journal of the Electrochemical Society, 163 (13) C752-C758 (2016)

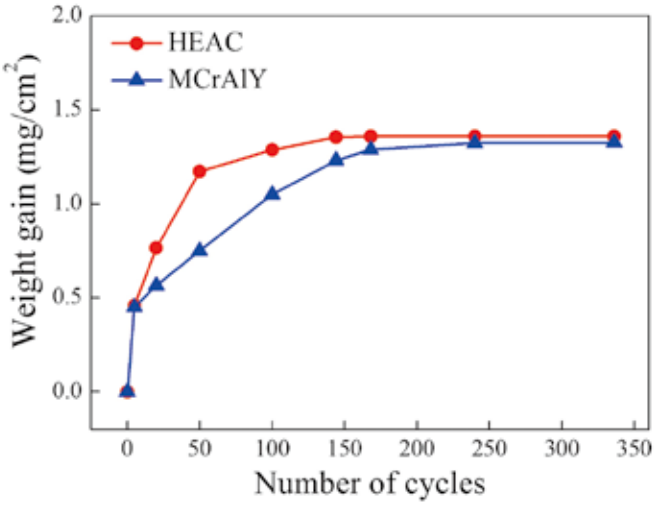

Fig. 1 Cyclic oxidation kinetics of SPS specimens for 1100°C cyclic test. HEAC displays very good oxidation resistance similar to that of MCrAlY

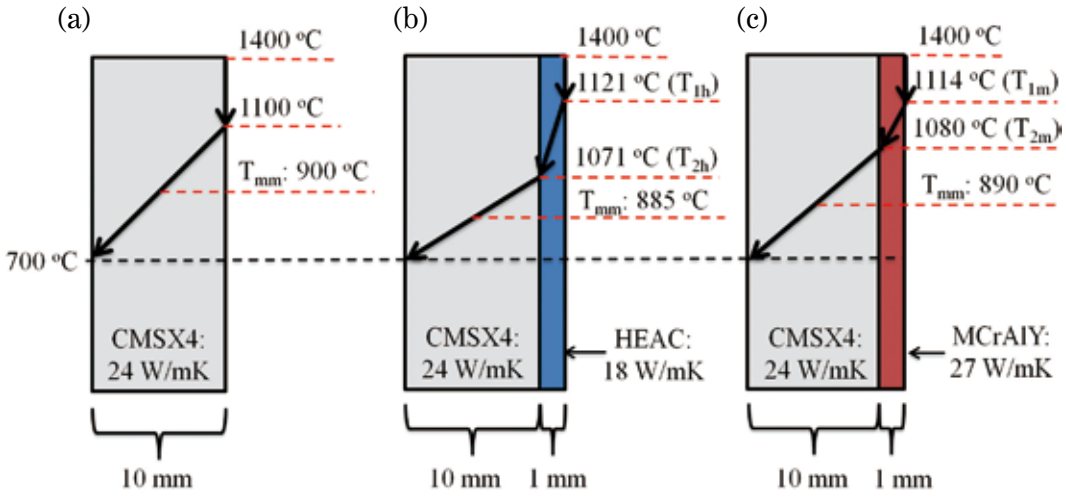

Fig. 2 Schematic of insulating effect of thermal barrier coating: (a) turbine blade, (b) turbine blade + HEAC coating, (c) turbine blade + MCrAlY coating. The heat insulation of TBC for turbine material will be improved by replacing MCrAlY to the HEAC.

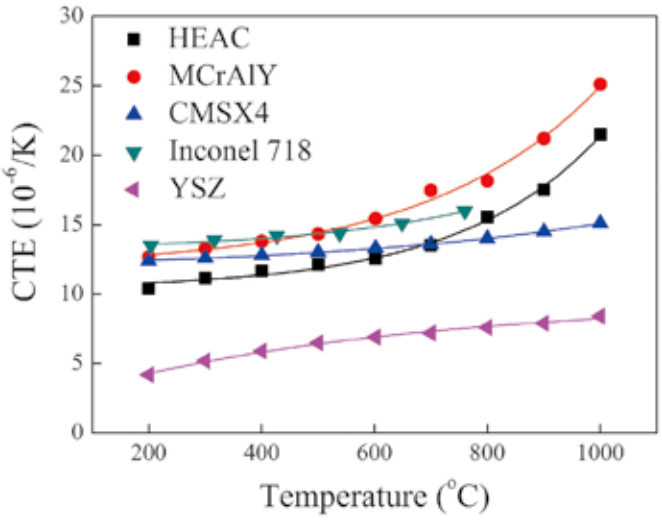

Fig. 3 CTE of different materials as a function of temperature. HEAC shows smaller thermal expansion and thus more compatibility to the blade alloys and YSZ top coat by reducing the interface stress and thus the stress induced effects such as buckling and cracking along the interfaces of YSZ/HEAC and HEAC/substrate, respectively.

Coating technology is critical for protecting components in gas turbine sections. The most advanced coating system is the thermal barrier coating (TBC), which contains a top coat of yttrium-stabilized zirconia (YSZ) and a compatible bond coat on the surface of the substrate. A bond coat can provide oxidation resistance and adhesion to an YSZ top coat, which offers thermal insulation and erosion resistance. Advanced bond coats are based on overlay coating compositions such as MCrAlY (M=Co, Ni), which is commonly used in industry to protect components at high temperatures. However, these overlay coatings have insufficient hardness and wear resistance at elevated temperatures, and the inter-diffusion between the coating and the substrate can result in detrimental secondary reaction zones. The present study proposes a new type of overlay coating based on the high-entropy alloy composition $NiCo_{0.6}Fe_{0.2}Cr_{1.5}SiAlTi_{0.2}$ [high-entropy alloy coating (HEAC)]. Both as-sintered specimens exhibit highly dense structure but the HEAC has a density smaller by 16.8%. The HEAC exhibits very high hardness (1045 Hv) at room temperature and a hot hardness of 230 Hv at 1100°C whereas the hardness of MCrAlY dropped from 450 Hv to 55 Hv. During the cyclic oxidation treatment at 1100°C up to 336 cycles, the HEAC displays very good oxidation resistance similar to that of MCrAlY because a continuous α-Al_2O_3 protective layer is also generated on top of the coating surface. In addition, the HEAC possesses a thermal conductivity lower than MCrAlY by 30% at 1000°C. The heat insulation of TBC for turbine material would be improved by replacing MCrAlY to the HEAC. HEAC shows smaller thermal expansion and thus more compatibility to the blade alloys and YSZ top coat by reducing the interface stress and thus the stress induced effects such as buckling and cracking along the interfaces of YSZ/HEAC and HEAC/substrate, respectively. Based on the above advantages, the investigated HEAC would be a promising overlay coating for high-temperature applications.

Authors

Wei-Lin Hsu, Hideyuki Murakami, Jien-Wei Yeh (葉均蔚), An-Chou Yeh, Kazuya Shimoda
http://jes.ecsdl.org/content/163/13/C752

The Electric Vehicle Touring Problem

Prof. Chung-Shou Liaoa
Department of Industrial Engineering and Engineering Management

Transportation Research Part B: Methodological Volume 86, 2016, pp. 163–180

Transportation is one of the fastest-growing sources of greenhouse gas emissions that contribute to climate change. In the last decade, the automobile industry has developed an increasing number of electric (battery) vehicles or hybrid electric vehicles to deal with the rising cost of energy. Electric vehicles (EVs), which release almost no air pollutants, could make a significant contribution to maintaining the quality of the environment. Briefly, EVs have the potential to reduce the greenhouse effect and facilitate more efficient use of energy resources. In particular, an efficient EV routing service would obviously encourage the transition to electric vehicle use.

Due to such increasing concern over global warming, which has led to the rapid development of the electric vehicle industry, we consider several EV route planning problems that take into consideration possible battery charging or swapping operations. Given a road network, the objective is to determine the shortest (travel time) route that a vehicle with a given battery capacity can take to travel between a pair of vertices or to visit a set of vertices with several stops, if necessary, at battery charging or switch stations.

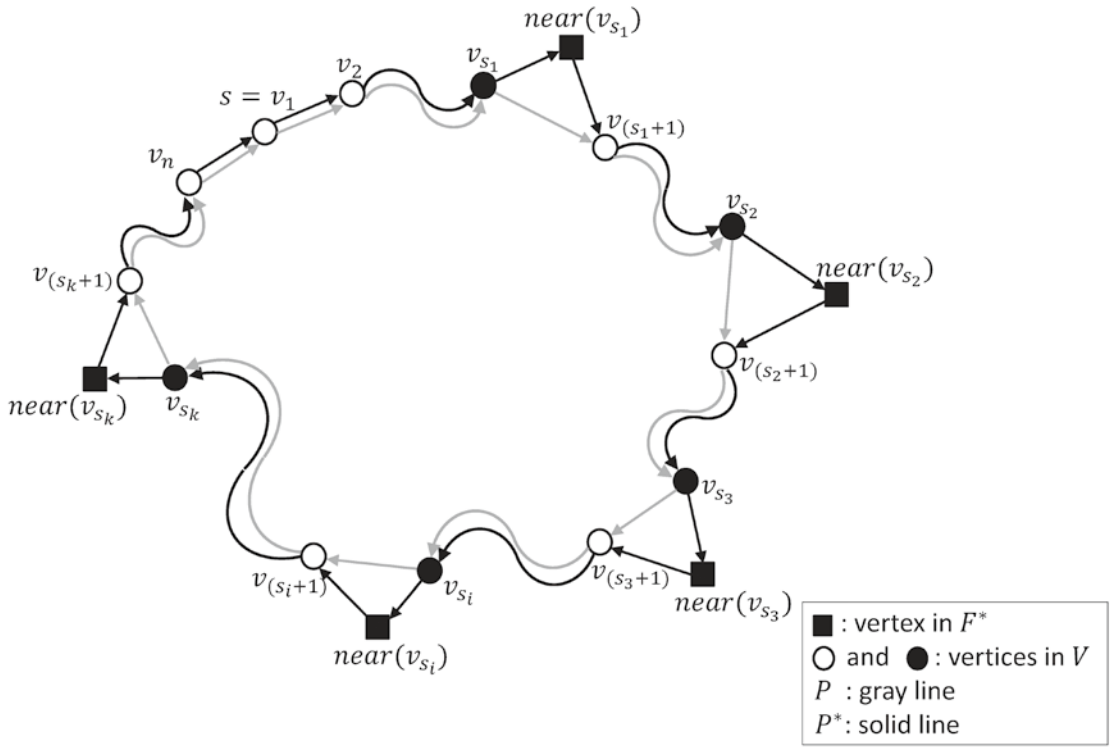

Fig. 1. An example illustrating the graph transformation from the EV touring problem

It is actually difficult to design an optimal EV route planning service because EVs have some serious limitations. The first is the low energy capacity of batteries. Currently, their common range is only 150 to 200 kilometers; hence, EVs are used primarily in urban areas. The second problem is that EV batteries require a long charging time. At the moment, they can be fully recharged from empty in 2 to 6 hours, depending on the level of charging available at the station. These factors have delayed the growth of the EV market; however, EVs can now be refueled in a matter of minutes through a system called battery-swaps. Recently, Tesla Motors and Gogoro Scooter Company provided the solution via a network of battery switch stations. The state-of-the-art technology leads to a new mathematical model of EV route planning.

In this study, we thus investigated the electric vehicle routing problem and provided solutions to determine the shortest route for electric vehicles with the latest battery charging operation, i.e. battery-swaps. More precisely, we present polynomial time algorithms for the EV shortest travel time path problem and the fixed tour EV touring problem, where the fixed tour problem requires visiting a set of vertices in a given order. We also propose constant factor approximation algorithms for the EV touring problem, which is a generalization of the traveling salesman problem. Note that the above results were derived based on a transformation from the EV touring problem to a combinatorial optimization problem in circular-arc graphs.

Finally, the implementation of these approximation algorithms were conducted to develop an online EV routing service via Google Map. The result has been published in the topmost journal in the field of transportation: Transportation Research Part B: Methodological. Moreover, this paper has been recognized as Yuan-Ze Hsu Science Paper Award in 2017.

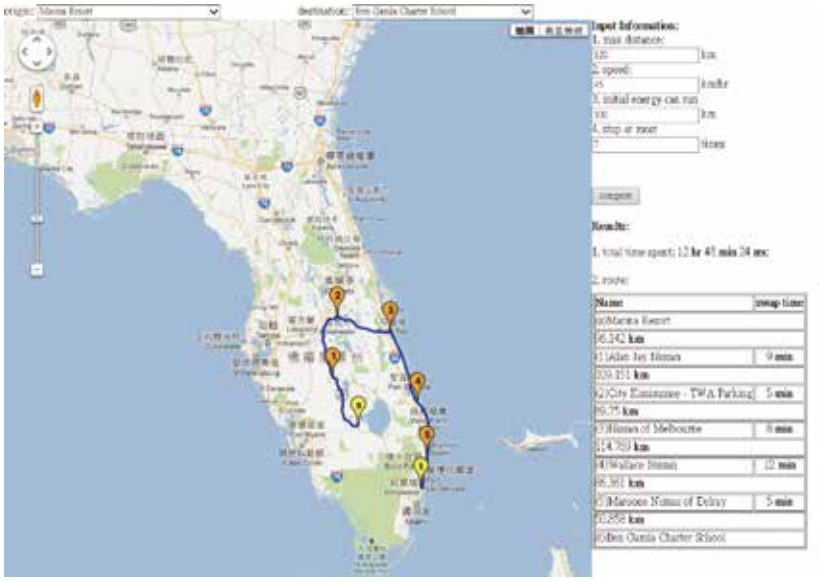

Fig. 2. An implementation the proposed algorithm in Florida, USA

Authors

Chung-Shou Liaoa (廖崇碩), Shang-Hung Lua, Zuo-Jun Max Shen
https://doi.org/10.1016/j.trb.2016.02.002

An Outline of the Grammar of the Ancient Chinese

Prof. Kuang Mei
Institute of Linguistics

Sanmin Books, Taipei 2015

This book is a collection of the author's long-standing thinking and researching of the grammar of Chinese. It is up to date the most complete and comprehensive work of the system of the Ancient Chinese grammar by the author. The writing is easy to follow yet sophisticated in content, and the focus is fairly put on both the theoretical and the empirical aspects of the phenomena. The book therefore has a sound theoretically basis, and successfully demonstrates the characteristic features of the Ancient Chinese. It is hoped that this book contributes to both the learning of the Ancient Chinese and its linguistic research.

Kuang Mei, Professor Emeritus of Linguistics, for receiving the 2016 Academic Award from the Ministry of Education, Taiwan

Authors

Kuang Mei (梅廣)
http://m.sanmin.com.tw/product/index/005044869

Hepatitis B virus PreS2-mutant large surface antigen activates store-operated calcium entry and promotes chromosome instability

Prof. Lily Hui-Ching Wang
Institute of Molecular and Cellular Biology

Oncotarget, 2016, 7(17):23346-60

Hepatitis B virus (HBV) is a driver of hepatocellular carcinoma, and two viral products, X and large surface antigen (LHBS), are viral oncoproteins. During chronic viral infection, immune-escape mutants on the preS2 region of LHBS (preS2-LHBS) are gain-of-function mutations that are linked to preneoplastic ground glass hepatocytes (GGHs) and early disease onset of hepatocellular carcinoma. The pathological mechanism leading to the development of this particular GGHs is not yet identified. In this study, we have explored such mechanism and demonstrated that disturbance of intracellular calcium homeostasis by store-operated calcium entry (SOCE) is the major cause for the formation of GGHs. In addition, the activation of SOCE also contribute to subsequent genome instability, thereby provoking hepatocarcinogenesis in patients with chronic HBV infection.

During chronic HBV infection, viral surface antigen (HBsAg) is the most abundant viral product detected in the liver and circulation in patients. The surface antigen gene contains three segments (preS1, preS2, and S) with two internal translation start sites that produce three polypeptides with a common C-terminus: large (LHBS), middle (MHBS), and small surface antigens (HBS). Clinical assessment of HBsAg usually uses antibodies specific for the common S region to detect all three types of HBsAg. In early stages of chronic HBV infection, HBsAg exhibits diffused cytoplasmic distribution in the liver. Occasionally, hepatocytes expressing inclusion-like HBsAg, known as type I ground glass hepatocytes (GGHs), can be found. In advanced disease, histological preneoplastic changes are detected in clusters of hepatocytes with a specific marginal distribution of HBsAg, known as type II GGHs or marginal type GGHs (Figure-1). Notably, the development of different GGHs reflects the emergence of immune-escape mutants during chronic viral infection. In addition, approximately 45% to 60% of HCC patients had preS mutants, suggesting these mutations are gain-of-function mutations during hepatocarcinogenesis. In-frame truncations of the immune-dominant preS2 region with or without a preS2 start codon mutation were isolated from type II GGHs using laser capture microdissection and in the serum of patients with advanced liver diseases and HCC. These studies implied that preS2 truncation mutants are immune-escape gain-of-function mutations that contribute to the development of HCC during chronic HBV infection.

In this study, we have explored whether the subcellular distribution of preS2-LHBS is essential for its oncogenic properties during disease progression. Unlike conventional

ER-resident proteins that display typical perinuclear distribution in the cell, preS2-LHBS was mostly detected at the cell margin in type II GGHs and HuH-7 cells following transient transfection (Figure-1). we show that the expression of preS2-LHBS increased ER and plasma membrane connections through the activation of store-operated calcium entry (SOCE), which is mediated by the interaction between stromal interaction molecule-1 (STIM1) and a calcium release-activated calcium modulator 1 (Orai1) (Figure-2). The activation of SOCE not only increased the intracellular calcium concentration but also provoked centrosome overduplication. By time-lapse imaging, hepatocytes carrying preS2-LHBS underwent aberrant multipolar division and ultimately reached chromosome aneuploidy. Finally, we show that preS2-LHBS is capable of inducing xenograft tumorigenesis, and this effect was largely suppressed by the depletion of STIM1. Thus, we suggest that the activation of SOCE machinery is involved in chromosome instability in the development of HBV-mediated HCC (Figure-3).

Notably, the activation of SOCE machinery explains the marginal recruitment of preS2-LHBS and the subsequent chromosome instability. To the best of our knowledge, this study provides the first mechanistic link between calcium homeostasis and chromosome instability in the pathogenesis of HBV. Notably, SOCE was shown to be essential for the migration, invasion, and proliferation of hepatoma cells and cervical carcinoma. Together, these studies highlight SOCE as a promising therapeutic target to control disease progression during chronic HBV infection.

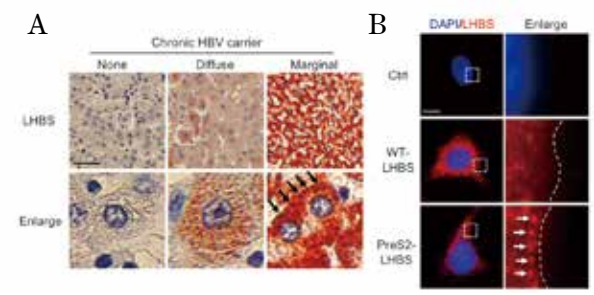

Fig.1 Intracellular distribution of LHBS in the liver (A) and in hepatoma cells (B).

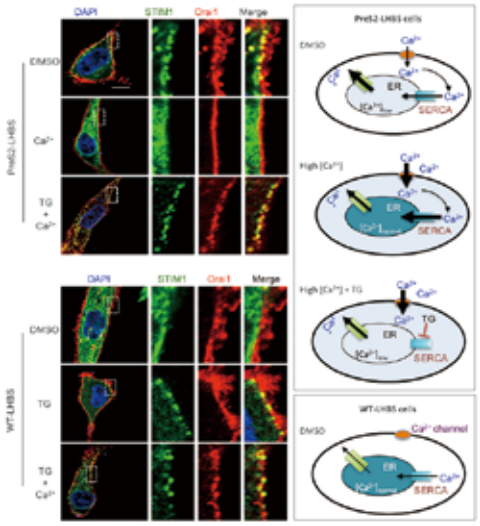

Fig.2 Activation of SOCE depends on the calcium concentration in the ER.

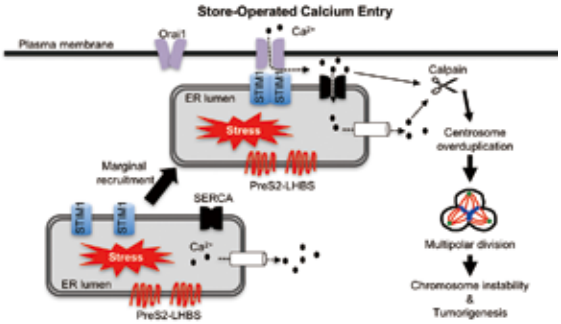

Fig.3 Cause and consequences of persistent ER-PM connections in type II GGHs.

Authors

Yen TT, Yang A, Chiu WT, Li TN, Wang LH, Wu YH, Wang HC, Chen L, Wang WC, Huang W, Chang CW, Chang MD, Shen MR, Su IJ, Wang LH
http://www.impactjournals.com/oncotarget/index.php?journal=oncotarget&page=article&op=view&path%5B%5D=8109

Asynchronous Quorum-Based Blind Rendezvous Schemes for Cognitive Radio Networks

Prof. Jang-Ping Sheu
Department of Computer Science

IEEE Transactions on Communications 64.3 (2016): 918-930.

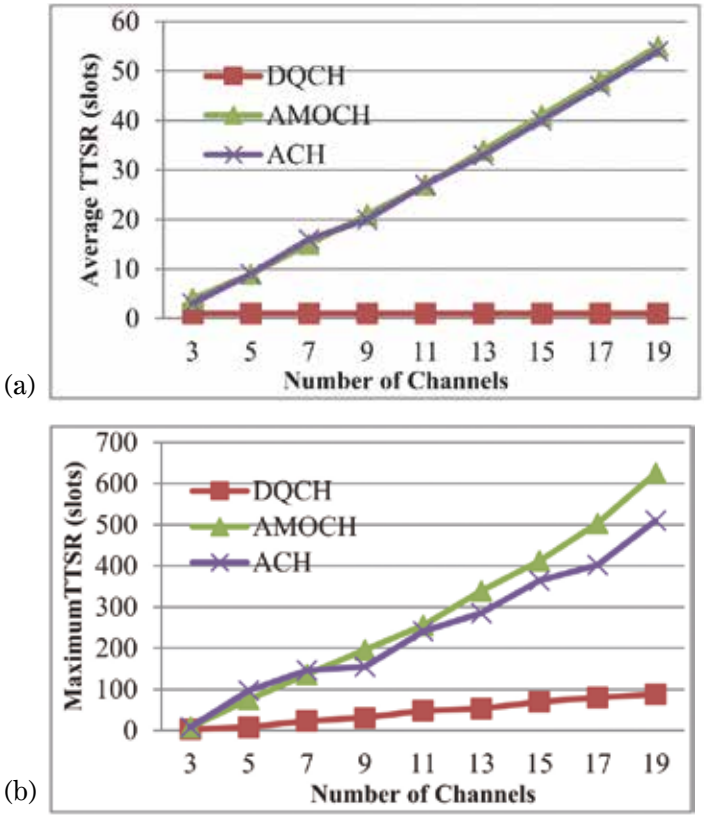

Fig.1 TTSR vs. the number of PUs in asymmetric-role environments.

In cognitive radio networks, unlicensed users secondary users (SU) need to rendezvous on licensed channels before establishing communication links. Dedicated common control channel is the simplest way to achieve rendezvous. However, due to the absolute priority of licensed users [primary users (PU)] on accessing licensed channels, a dedicated common control channel may cause the PU long-time blocking problem, and the control channel saturation problem in a high SU density environment. Channel hopping (CH) schemes have been proposed to avoid the problems mentioned above.

In this research, we study asynchronous CH approaches. Existing asynchronous CH approaches usually have one or more of the following drawbacks: unbounded/long Maximum Time-to-Rendezvous (MTTR) and Maximum Conditional Time-to-Rendezvous (MCTTR), high/unbalanced channel loading, and low degree of rendezvous. We proposed two quorum-based CH protocols for asynchronous environments: one asymmetric-role approach, Dynamic asymmetric-role Quorum-based Channel Hopping (D-QCH), and one symmetric-role approach, Symmetric-role Quorum-based Channel Hopping algorithm(S-QCH). To reduce MCTTR, each D-QCH/S-QCH sequence is determined according to the detected available channels. D-QCH has smaller MCTTR = $(\alpha - k + 1)$N, where α is the number of channels available to the receiver and k is the number of channels commonly available to sender and receiver. S-QCH has MCTTR = $(\alpha - k + 1)N(2N + 1)$, where α is the number of channels available to a SU.

In the simulations, the number of SUs is fixed at 50 and the number of PUs varies from 0 to 100. Since high PU density leads to fewer available channels, SUs usually need more time to rendezvous on an available channel, i.e., the time-to-successful-rendezvous (TTSR) increases as the number of PUs increases. Fig. 1(a) shows the average TTSR of D-QCH, ACH, and A-MOCH. When PU density is low, DQCH has TTSR shorter than that of ACH and A-MOCH since D-QCH has small MTTR. The number of PUs has a rather less negative impact on D-QCH. This is because D-QCH would skip unavailable channels (i.e., the probability of an SU staying at an available channel increases) and thus the probability of two neighboring SUs staying at the same available channel increases, especially when PU density is high. Fig. 1(b) shows the maximum TTSR. ACH and A-MOCH have nearly the same maximum TTSR because they have the same MCTTR.

In this paper, we have introduced two asynchronous quorum-based CH protocols for CRNs. For asymmetric-role environments, D-QCH has the maximum degree of rendezvous among commonly available channels, and excellent MTTR and MCTTR. By dynamically changing the CH period, D-QCH reduces the time-to-rendezvous, especially when available channels are few. For symmetric-role environments, S-QCH has the maximum degree of rendezvous, balanced channel loading, and excellent MCTTR. According to our simulations, D-QCH has performance better than previous work, while S-QCH outperforms in environments with high PU density or high SU traffic volume.

Authors

MLA Sheu, Jang-Ping (許健平), Chih-Wei Su and Guey-Yun Chang
http://ieeexplore.ieee.org/stamp/stamp.jsp?arnumber=7355336

A 5.28-Gb/s LDPC Decoder with Time-Domain Signal Processing for IEEE 802.15.3c Applications

Prof. Yeong-Luh Ueng
Department of Electrical Engineering

IEEE JOURNAL OF SOLID-STATE CIRCUITS, VOL. 52, NO. 2, pp. 592-604, FEB 2017

This paper presents a high-throughput, energy-efficient, and scalable low-density parity-check (LDPC) decoder with time-domain (TD) signal processing. The proposed arbiter-based minimum value finder as shown in Fig. 1 is able to support practical long codes. The latency for determining the first two minimum values required in the check node unit is significantly reduced through TD processing. A layered Q-based decoding architecture together with the variable-node unit (VNU) is proposed in order to reduce the amount of memory used for check node storage, as shown in Fig. 2 and Fig. 3. Multimode operations are supported by leveraging the structure of the base matrices and the proposed scalable minimum finder architecture.

As a proof of concept, a TD-based multimode LDPC decoder for high-speed IEEE 802.15.3c is designed and fabricated in a 90-nm CMOS process. The microphotograph of the LDPC decoder chip is shown in Fig. 4. The decoder integrates 495k logic gates in 2.25 mm^2 and achieves a throughput of 5.28 Gb/s at 157 MHz from a 1.05 V supply voltage. The power and normalized energy dissipation are 182 mW and 34.47 pJ/b, respectively. The proposed LDPC decoder is more hardware and energy efficient than previous digital counterparts and is able to support long codes for practical applications, which is still infeasible for the state-of-the-art TD-based LDPC decoders

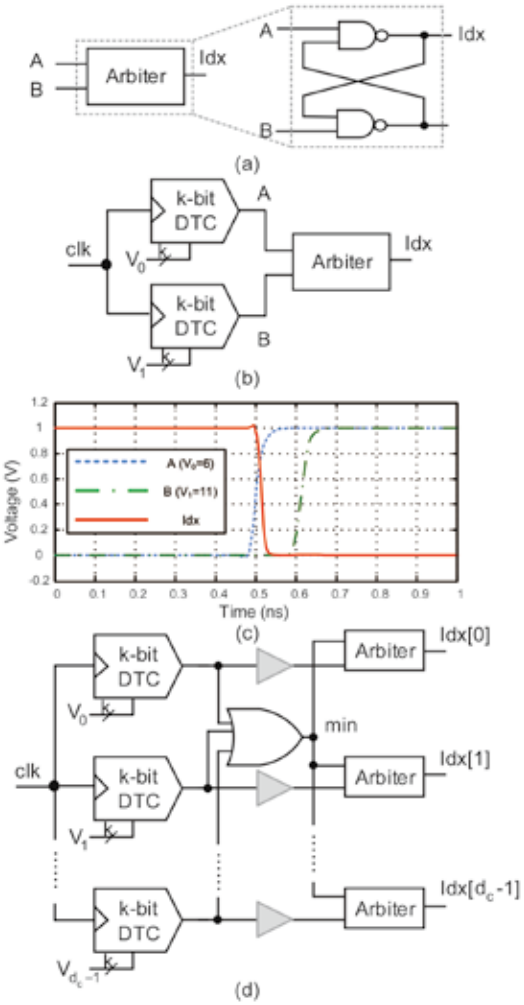

Fig. 1. (a) Arbiter circuit diagram. (b) Block diagram of a two-input TD comparator. (c) Simulation waveforms of the two-input TD comparator. (d) Block diagram of the minimum index generator with d_c inputs. The matching cells are shaded in gray.

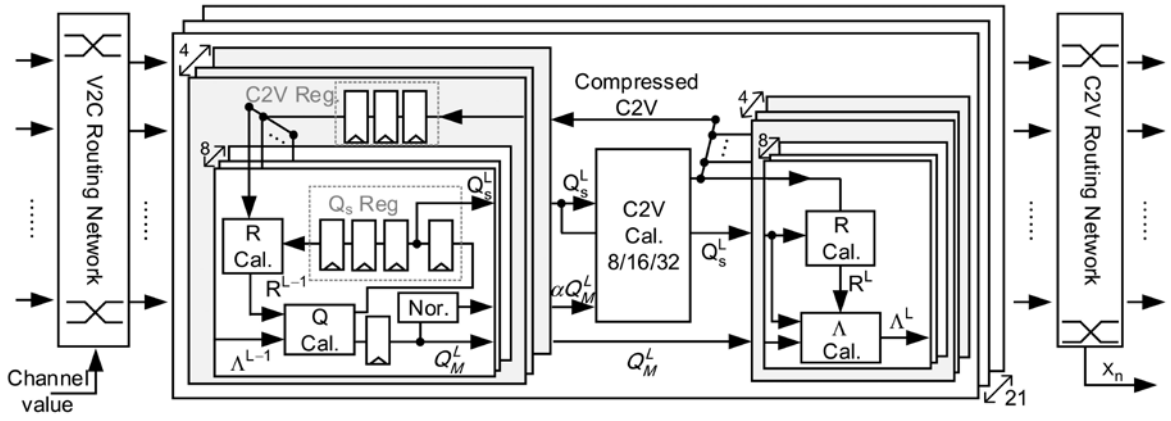

Fig. 2. Architecture of the proposed multi-rate TD LDPC decoder. An LDPC decoder for IEEE 802.15.3c applications is designed so as to demonstrate the proposed TD signal processing techniques and related circuits. In order to facilitate the TD signal processing, a *Q*-based layered decoder architecture is proposed. Furthermore, MVIG, CNU, and outing networks are properly tailored in order to support the requirements of multimode operations specified in the IEEE 802.15.3c standard.

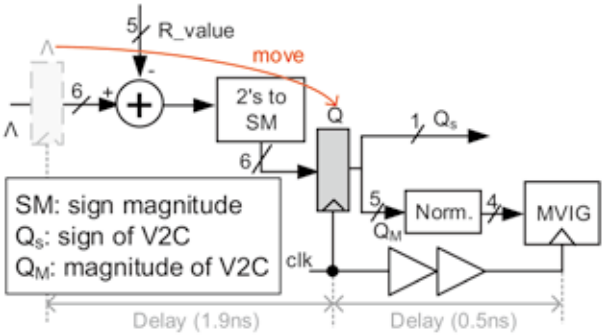

Fig. 3. Proposed Q-based VNU architecture. In order to reduce the area of the delay controller, a Q-based VNU architecture is proposed, where the V2C messages, i.e., Q_{mn}, are stored rather than the Λ values. Simulation results show that the delay can be reduced to 0.5ns, translating into an improvement in the operating frequency of 4.6 times.

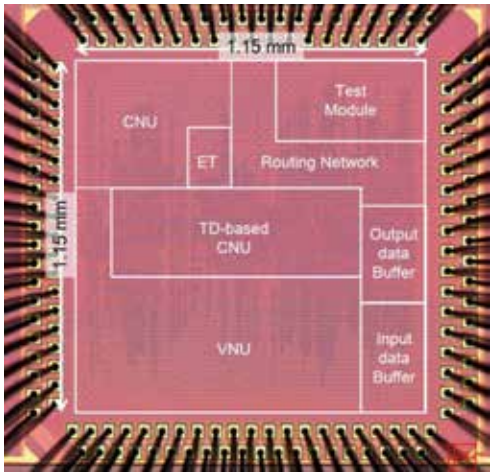

Fig. 4. Microphotograph of the LDPC decoder chip. The chip includes an LDPC decoder, a test module, and input/output data buffers in a core area of 2.25 mm^2.

Authors

Mao-Ruei Li, Chia-Hsiang Yang, and Yeong-Luh Ueng (翁詠祿)
http://ieeexplore.ieee.org/document/7765065/

Exemplary Achievements

A disposable breath sensing tube with on-tube single-nanowire sensor array for on-site detection of exhaled breath biomarkers

Prof. Chien-Chong Hong
Department of Power Mechanical Engineering

Lab Chip, 2016, 16, 4395

(a)

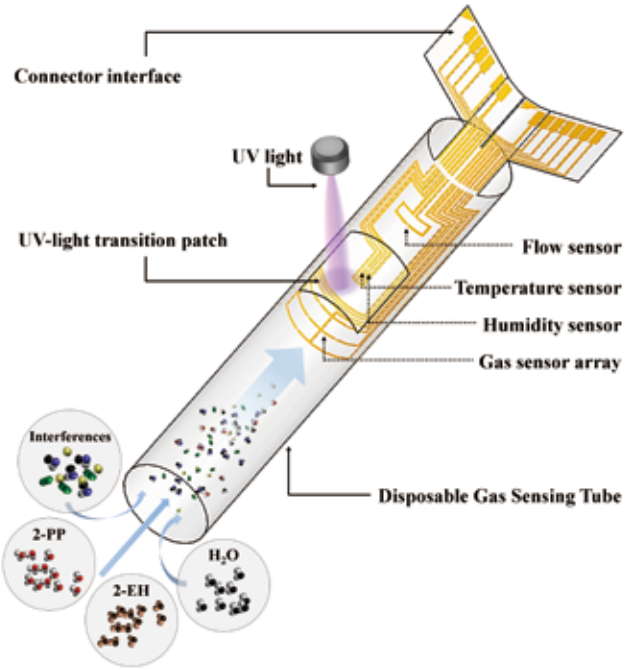

(b)

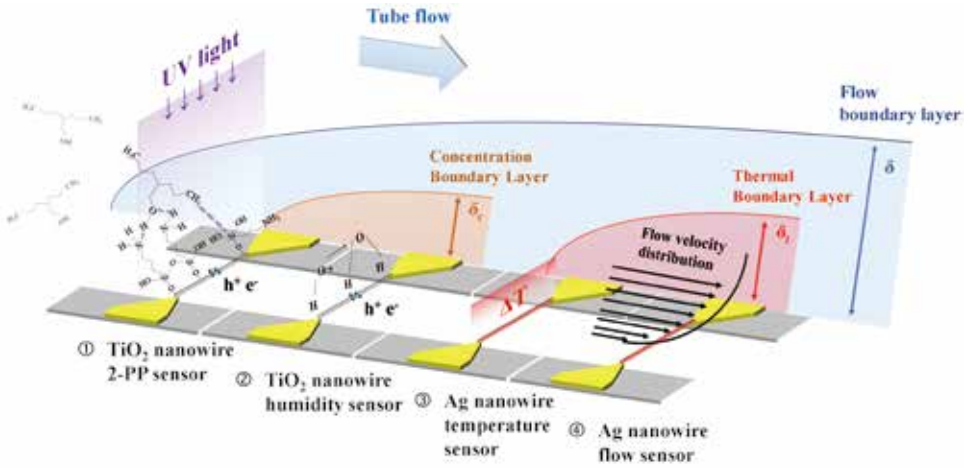

Fig. 1 Scheme of the proposed disposable breath-sensing tube and the sensing mechanisms. (a) Plastic tube with an on-tube NW sensor array for real-time detection in flowing gas, and (b) sensing mechanisms of the on-tube NW sensor array using single TiO_2 and Ag NWs fabricated and integrated with a flexible plastic substrate for lung cancer biomarkers and changes in the humidity, flow-rate, and temperature conditions of flowing gas.

This paper presents a novel disposable breath-sensing tube with an on-tube single-nanowire (NW) sensor array for noninvasive, simple, and on-site detection of exhaled breath biomarkers. Although various noninvasive detection methods for lung cancer biomarkers in breath samples, they are unsuitable for self-diagnostics and immediate detection because they entail complicated handling procedures and are time intensive. In this study, we simulated, fabricated, and characterized disposable nanosensors by using single TiO_2 and Ag NWs in flexible plastic tubes. The proposed sensors simultaneously detect 2-propyl-1-pentanol (2-PP) lung cancer biomarkers and changes in the humidity, flow rate, and temperature of the flowing gas. The optimal dimension of the tubes was determined and verified through dynamic simulations and experiments. The current tube design decreases sensing variation and moisture interference by 43.28% and 78.77%, respectively, compared with previous designs. In the future, the proposed breath sensor, which has a response time of less than 10 s, can be used in a tube for simple and quick screening of lung cancer patients with the 2-PP concentration exceeding 100 ppb. This novel disposable breath-sensing tube with an on-tube single-NW sensor array was developed for noninvasive, simple, and on-site detection of lung cancer biomarkers. The plastic tube with on-tube single-NW sensors demonstrates the advantages of low cost, fast response, and an easy-to-use breath-sensing procedure.

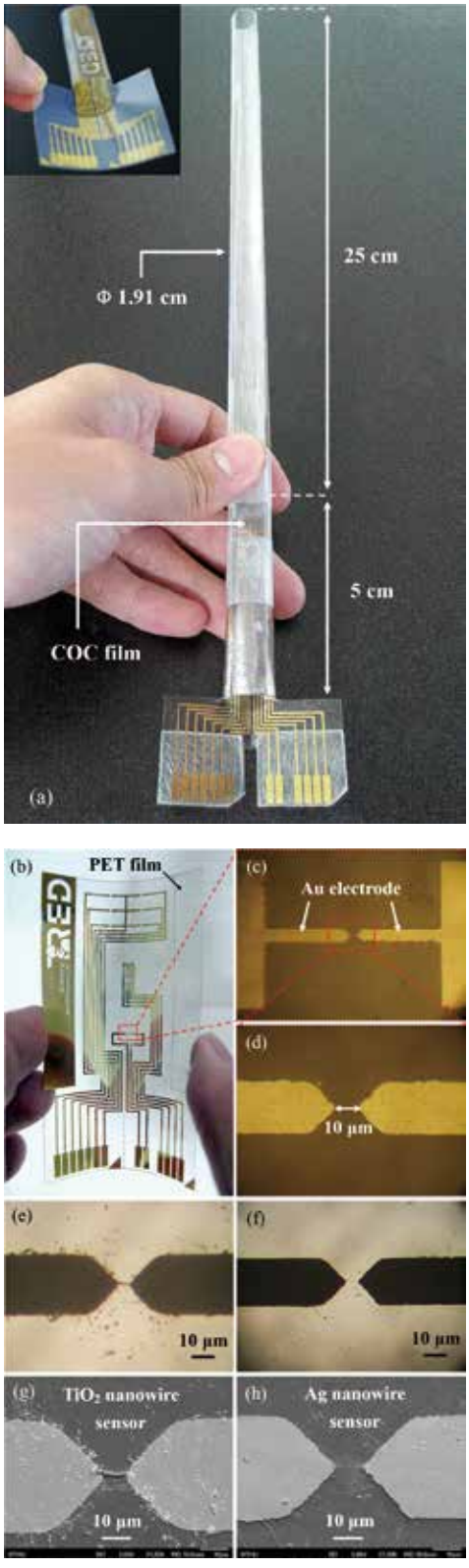

Fig. 2 Images of the developed gas-sensing tube and on-tube NW sensor array. Optical images of the (a) disposable gas-sensing tube, (b) flexible electrode array, (c) microelectrode for NW DEP assembly, (d) microelectrode (highly magnified), (e) DEP-assembled single TiO2 NW, and (f) DEP-assembled single Ag NW. Scanning electron microscope (g) image of the DEP-assembled single TiO_2 NW, and (h) DEP-assembled single Ag NW.

Authors

Chung-Hsuan Wu, Wei-Han Wang, Chien-Chong Hong (洪健中) and Kuo Chu Hwang
https://doi.org/10.1039/C6LC01157H

Electric Hum Signal Readout Circuit for Touch Screen Panel Applications

Prof. Chih-Wen Lu
Department of Engineering and System Science,

IEEE/OSA Journal of Display Technology, vol. 12, no. 11, pp. 1444-1450, November, 2016.

This paper presents a new touch sensing mechanism that detects different signals on a touch panel generated by an electric field formed from household power. Without requiring complicated transmitter and receiver circuits, a 16-channel front-end sensor and shared readout circuits are proposed to realize the new touch sensing mechanism. This touch sensing technique can be applied on the appliance control panel to detect the operation control.

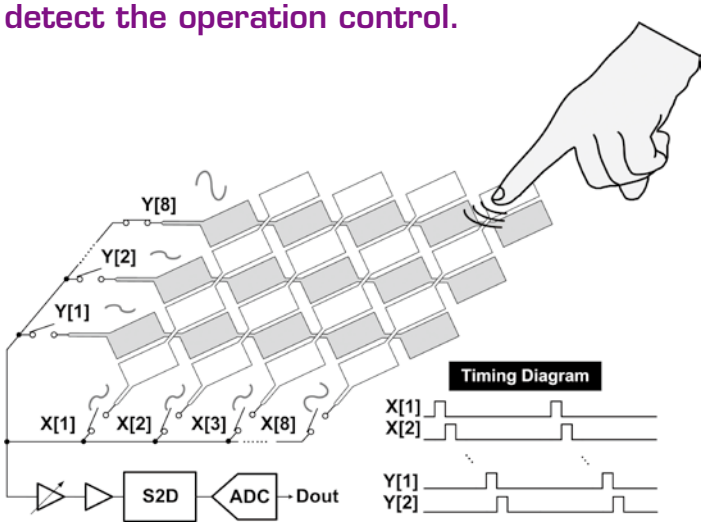

Fig. 1 Proposed electric hum signal readout circuit for touch screen panel

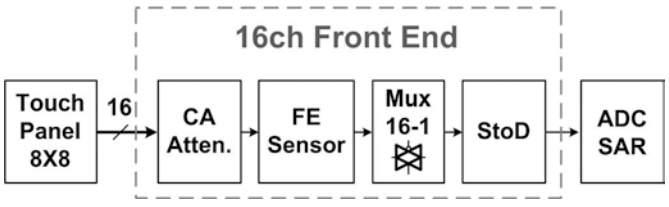

Fig. 2 System block diagram

Fig. 1 shows the operating scheme of the proposed electric hum signal readout circuit. When a finger comes close to the touch sensor panel, the coupled AC signal interacts with the touch sensor panel. The front-end circuit detects a stronger signal through the channel that the finger is closest to.

Fig. 2 shows the system block diagram of the proposed floating-sensing controller. The signal acquisition procedure is line-by-line scanning. There are eight rows of X-axis touch sensors and eight columns of Y-axis touch sensors. A total of 16 touch sensors are thus used to receive frame data. Through a comparison of the peak-to-peak value of the waveform data of each channel, the touch location can be detected.

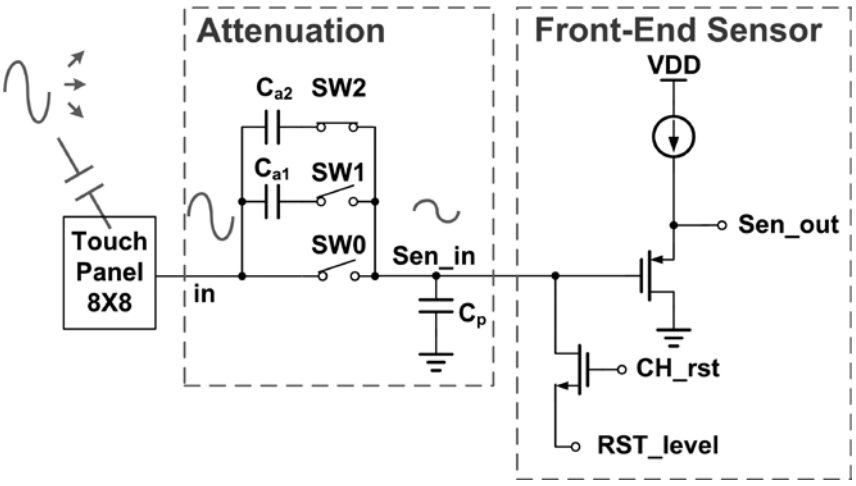

Fig. 3 Circuit diagram of front-end

Fig. 3 shows the circuit diagram of the proposed front-end circuit, which consists of two parts. The amplitude of the sinusoidal wave represents the distance between objects and the touch panel. When an object, in this case a finger, comes close to the panel, the amplitude of the front-end output increases. The first part of the front-end circuitry is the attenuation circuit, and the second part is front-end sensor. The second part of the front-end circuitry is the front-end sensor; which has two operating modes. When this channel is in reset mode, the input of the sensor is reset to a direct current (DC) level and the output is maintained at a DC value. When each reset signal, (CH_rst), is controlled by each channel, the background noise is greatly reduced and the signal-to-noise ratio is greatly enhanced.

The signal readout circuit is implemented in a 0.18-μm CMOS process, occupied an area of 2.64 mm^2. Fig. 4 shows the die micrograph of the 16 channels readout circuit. The proposed sensing technique achieves 46.5-dB signal-to-noise ratios with finger touch. With battery power supply of 1.8V and 2.5V, total power consumption of the proposed readout circuit is measured as just 2mW.

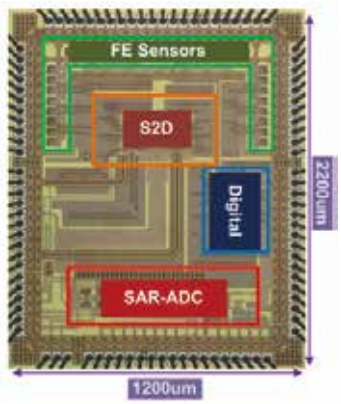

Fig.4 Die micrograph for the 16 channels readout circuit

Authors

Pei-Yi Lai Lee, Chih-Wen Lu (盧志文), Chih-Cheng Hsieh, Tsin-Yuan Chang, Jenny Yi-Chun Liu, Hsin-Chin Liang, and Hsiang-Ning Wu
http://ieeexplore.ieee.org/stamp/stamp.jsp?tp=&arnumber=7563339

Rookies and seasoned recruits: How experience in different levels, firms, and industries shapes strategic renewal in top management

Prof. Pao-Lien Chen
Institute of Technology Management

Strategic Management Journal, 38(7), 1391-1415

Who are in the talent market?

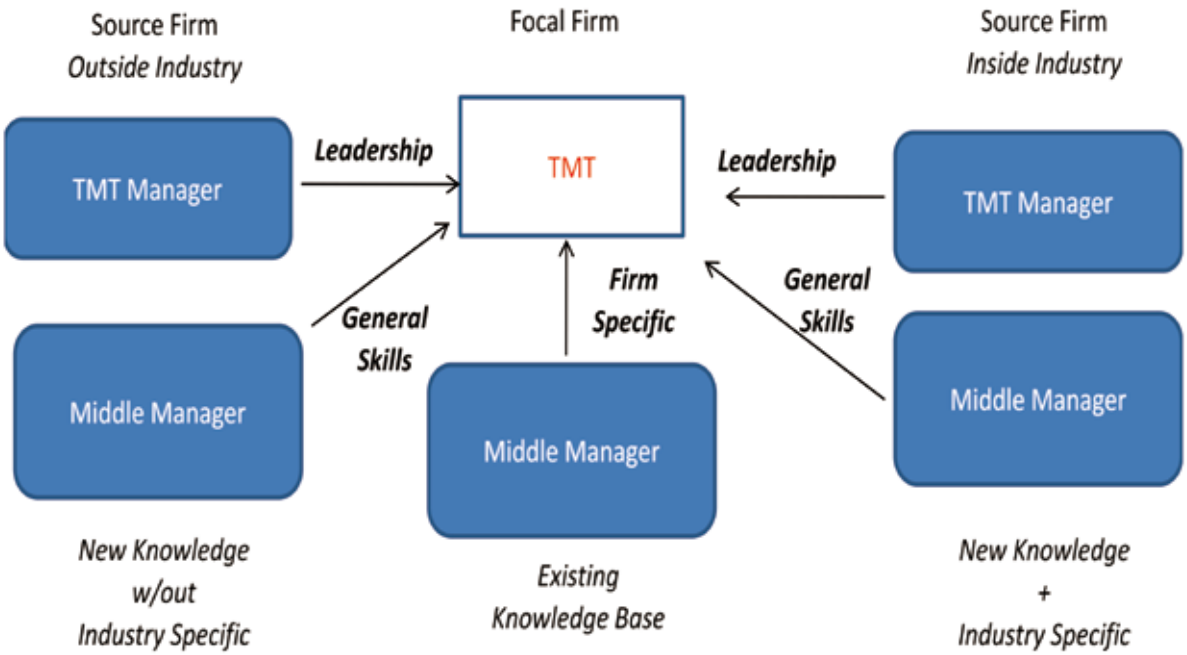

Managerial heterogeneity caused by differences in Hierarchical, Organizational, and Industrial origins

Research summary: This study explores the effect of knowledge integration on strategic renewal. In particular, it examines how executives from different levels and sources influence renewal when added to top management teams (TMT). In contrast to prior work, the study hypothesizes and finds that new outside rookies—those new to top management and the firm—are associated with higher firm growth than other types of executives. We also find that seasoned outsiders—those with prior TMT experience outside the focal industry—contribute to growth only when the existing TMT has a long tenure. The results suggest that the ability of the TMT to integrate new members varies by executive type and has an important effect on incremental strategic renewal.

Managerial summary: Conventional wisdom holds that firms are better off hiring those who can demonstrate prior experience and skill in tasks as close as possible to the job. In the realm of the top management team (TMT), however, we find that many firms benefit from hiring rookies from other firms who are new to the top management team level. These candidates bring useful knowledge of the operations of competitors and other firms, and they are easier to socialize and integrate with the existing team. While more experienced senior leaders may bring valuable strategic knowledge, this study suggests that only top management teams with long shared experience can weather the disruption that they cause to realize the potential benefits.

Authors

Williams, C., Chen, P. L. (陳寶蓮), & Agarwal, R.
http://onlinelibrary.wiley.com/doi/10.1002/smj.2562/full

Shi (勢), STS and Theory: Or what can we learn from Chinese Medicine?

Prof. Wen-Yuen Lin
Center for General Education,

Science, Technology Human Value 42(3): 405–428.

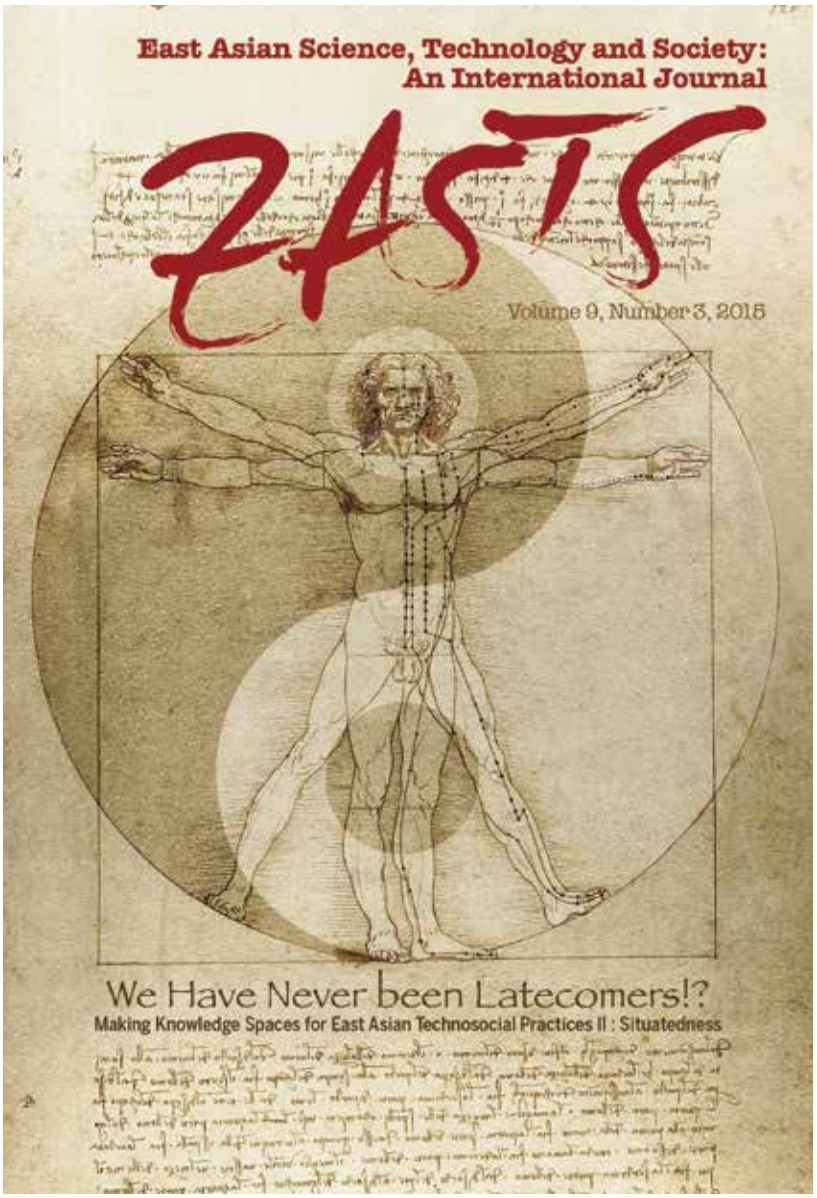

The picture is part of the joint works with this research, the cover of an edited special issue for EASTS by the author. It illustrates the possibility of exploring a new way of situated understanding in the conjuncture of the Easts, the West and the other possibilities.

How might STS learn from its studies of other knowledge traditions? This paper explores this question by looking at Chinese medicine (CM). The latter has been under pressure from modernization and 'scientization' for a century, and the dynamics of these pressures have been explored 'symmetrically' within STS and related disciplines. But in this work CM has been 'the case' and STS theory has held stable. This paper uses a CM term, reasoning-as-propensity (shi, 勢), to look at contemporary practices of cancer care in a hospital in Taiwan. It describes how shi (勢) informed the design of a new decoction, Kuan Sin Yin, whilst also relating to the production of scientific knowledge, biomedical interventions, Buddhist practices, and the patients living with cancer themselves. Does CM's use of shi (勢) simply confirm the essential and incompatible Otherness of CM? Looked at from outside the answer seems to be yes. However, this paper explores how STS might change itself –and the theory-practice division in STS – by thinking through shi (勢) in dialogue with its Othered object. This opens the possibility of an STS for CM.

This paper is part of a project aiming at exploring alternative ways of theorization from local intellectual resources and case studies. Please see also the following publications for more details:

- 林文源，2017，〈地方化後殖民：在地經驗、認識空間與實作本體論〉，《科技、醫療與社會》24:203-212。
- 林文源，2017，〈把疾病帶回來？病患實作中的多元疾病客體化〉，《台灣社會學》33: 1-62。
- Law, John* and Wen-yuan Lin, 2017, The Stickiness of Knowing: translation, postcoloniality and STS, East Asian Science, Technology and Society 11(2): 257-269.
- Law, John* and Wen-yuan Lin, 2017, Provincialising STS: postcoloniality, symmetry and method, East Asian Science, Technology and Society 11(2): 211-227.
- 林文源，2016，〈旅行的意義〉，《科技、醫療與社會》23:67-76。
- 林文源，2015，〈跟著 STS 去旅行〉，《科技、醫療與社會》21:9-13。
- 林文源，2015，〈正視在地知識空間：位移方案與理論化在地的問題性〉，《台灣社會學刊》，56:219-231。
- Lin, Wen-yuan* and John Law, 2014, A Correlative STS: Lessons from a Chinese Medical Practice, Social Studies of Science 44(6):801-824.

Authors

Lin, Wen-Yuen (林文源)
http://journals.sagepub.com/doi/full/10.1177/0162243916671202

Privatizing the Imperial Landscape: The Rise of Pictorial Autobiographies and Travel Memoirs in Early Nineteenth-Century China

Prof. Yun-chiu Mei
Center for General Education

Taida Journal of Art History, Vol. 41, pp. 303-370.

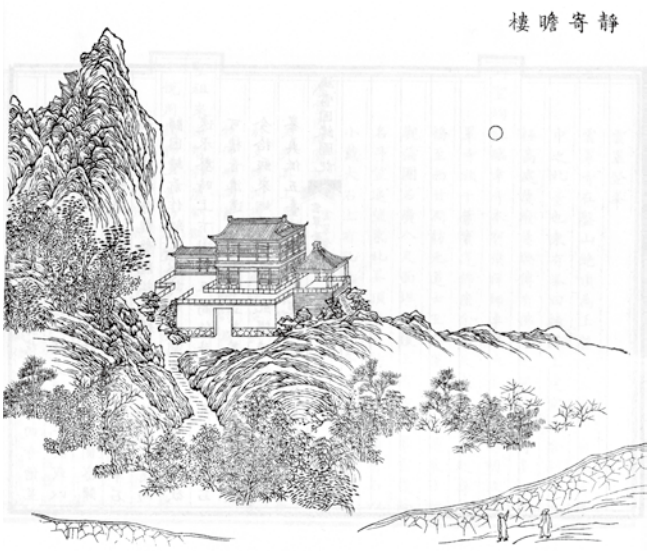

Fig. 1 An illustration from Linqing's *Tracks in the Snow* records his personal visit to the temporary palace constructed by the Qianlong emperor at Mount Pan in modern-day Tianjin.

During the early nineteenth century when the Qing empire (1644-1911) began to decline and the imperial court gradually reduced its sponsorship of art production, a new type of pictorial autobiography or travel memoir emerged. Produced either by government officials or local elites, it often contains personal and at times journalistic accounts of current events, government affairs, imperial spectacles as well as famous tourist sites across China. Through examining extant works of this type, including *Tracks in the Snow: An Illustrated Autobiography* by the Manchu governor-general Linqing (1791-1846), *Idle Talks of the Elderly* by the magistrate and poet Zhang Weiping (1780-1859) from Canton, and *Pictures of My Voyages* by Zhang Bao (b. 1763), a Nanjing literati painter who once served as a private secretary to Prince Li, I intend to locate a visual culture primarily created by bureaucrats and social elites outside the imperial court in the Jiaqing (1796-1820) and Daoguang periods (1821-1850). Among them, the resourceful provincial governor and governor-general along with their expending private bureaucracy, appear to be most aggressive and ambitious in taking over a cultural enterprise previously dominated by the imperial court, in particular, the Qianlong court (1736-1795).

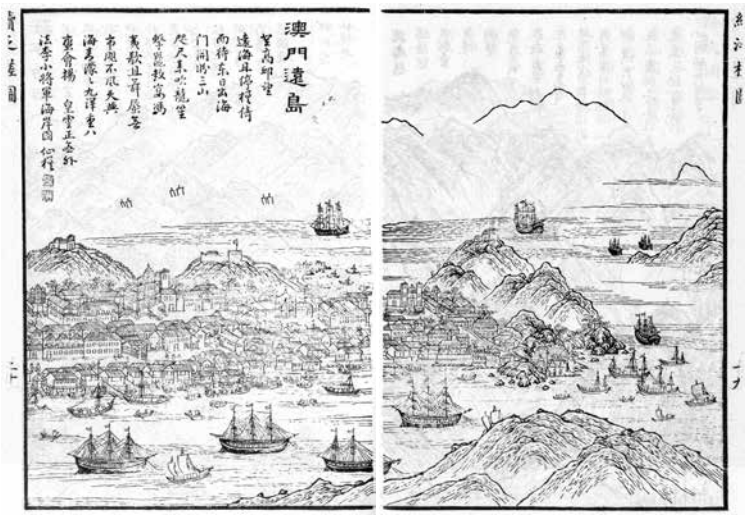

Fig. 2 An illustration from Zhang Bao's Pictures of My Voyages depicts a panoramic view of European buildings and foreign merchant ships in the Portuguese colony Macao.

Although prior to the Qianlong era, it was not unusual for government officials to employ pictorial biographies or memoirs as an alternative way of chronicling their personal histories and public services, I find that these biographical picture books produced in the earlier periods actually look quite different from their nineteenth-century counterparts. With an attempt to preserve the physical likeness of biographees or to dramatize their life stories, these earlier examples were usually executed by artists specializing in narrative figure painting or portraiture, whereas those created in the nineteenth century unequivocally prefer landscape as a representational vehicle to figure painting. In turn, the main focus of their renditions also shifts from human activities to actual places, many of which were significant to the lives and careers of the autobiographers, such as their offices, residences, family estates, ancestral cemeteries and hometowns. Meanwhile, in order to exhibit their extensive travel experience and geographical knowledge, these autobiographers were also keen to provide a comprehensive record of famous sites which they personally visited during their journeys through the empire. As a result, their visual memoirs could also stand out as an encyclopedic mapping of China's iconic landmarks despite the presence of some autobiographical elements.

It is worth noting that individual endeavors to compile and publish illustrated encyclopedias of iconic landmarks in China, which flourished especially in the late Ming (1368-1644), were swiftly interrupted or dissuaded following the foundation of the Qing. Throughout the eighteenth century, known as the golden age of Qing power, only those imperially sponsored compilation projects came to fruition. The aforementioned nineteenth-century privately-made compilations thus not only afford more personalized and diversified visual representations of the vast territories under Qing rule, but also epitomize the resurgence of individual efforts to launch ambitious cultural projects after a century long hiatus.

Authors

Mei, Yun-chiu (梅韻秋)
http://ejournal.press.ntu.edu.tw/record.php?Access_Num=569672&DataId=NTUJD00001430

Effective Assessment Models for Remedial Teaching and Interdisciplinary Education

Prof. Tzu-Hua Wang
Department of Education and Learing Technology

1. Science Education Research and Practice in Asia - Challenges and Opportunities (pp. 461-481). Dordrecht, The Netherlands: Springer.
2. EURASIA Journal of Mathematics, Science & Technology Education, 13(4), 1045-1058.
3. Chinese Journal of Science Education, 25(2), 143-168

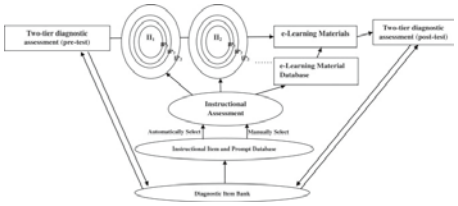

Fig1. GPAM-WATA_EL framework

Fig2. Annotated e-Learning materials. (A) Student can link to the learning materials. (B) Adaptive annotation

Effective Assessment Models for Remedial Teaching

With the development of information communication technology, digital assessment has become an important educational assessment mechanism. The theory of "assessment as a teaching and learning strategy (ATLS)" is proposed (Wang & Yang, 2016). It expects that in addition to evaluating learning effectiveness, assessment can play a more positive and effective role in teaching activities. Assessment has to be closely integrated with teaching activities to enable assessment to assist in teaching and developing learning strategies. Based on the idea of ATLS, the Graduated Prompting Assessment Module of the WATA system (GPAM-WATA) and the GPAM-WATA e-Learning system (GPAM-WATA_EL) are developed (Wang & Yang, 2016). In GPAM-WATA, test items play the role of instructional items. When examinees answer the items, the system provides them with graduated timely feedback, which includes the teaching and learning resources teachers provide. With the instructional prompts, examinees achieve learning by answering test items and receiving timely feedback. In GPAM-WATA_EL (Fig1), digital assessment can be administered with the combination of two-tier diagnostic test and dynamic assessment. The digital two-tier diagnostic test serves as a diagnostic assessment that identifies the learner's learning deficiencies. Using these, the system then automatically constructs a personalized dynamic assessment for learners to answer. By answering test items (i.e. instructional items) and receiving prompts (i.e. instructional prompts), examinees can improve their learning deficiencies. Based on examinee's performance in the two-tier diagnostic test and dynamic assessment, the system recommends digital learning materials for learners to enhance learning (Fig2). This design can effectively improve learner's learning achievement and reduce their misconceptions. It is especially significant in assisting learners with lower prior knowledge (Wang & Yang, 2016). It is also effective when applied to the remedial teaching of mathematics and science (Lin & Wang, 2017). GPAM-WATA_EL has been applied in mathematics and science teaching at several elementary and junior high schools in Taiwan.

Effective Assessment Models for Interdisciplinary Education in Higher Education

Interdisciplinary education provides students with opportunities to widely explore. Students are able to cooperate and interact with peers from other fields using their own professional knowledge and skills. Chen, Wang, Chiu, Shen, & Zeng (2017) developed an assessment mechanism for evaluating student interdisciplinary integration-based competencies (Fig3). It includes assessment of "shared interdisciplinary integration-based core competencies," "professional interdisciplinary integration-based core competencies," and "professional competencies in non-specialist fields." "Shared interdisciplinary integration-based core competencies" refer to the general competencies not related to professional fields, "professional interdisciplinary integration-based core competencies" refer to the competencies related to professional fields, while "professional competencies in non-specialist fields" refers to the specialties students should have in addition to the professional competencies of their major. "Shared interdisciplinary integration-based core competencies" can be applied across many subjects and fields. This concept is defined using three dimensions: (I) Communication: learners can listen to the opinions of people from different professional backgrounds, understand the terms they use, respect their professional opinions, conduct communication, and achieve consensus through communication tools. (II) Reflection: learners can reflect and generate new ideas in the process of interacting with others, understand the problems encountered during completing tasks, and actively search for possible solutions. (III) Implementation: learners can complete group tasks by working with people with different professional backgrounds and modify their own viewpoints through interaction with peers. They can evaluate the administration effectiveness of group solutions for the problems encountered, and actively assess group work efficiency. Based on the maternal-infant life services interdisciplinary talent cultivation for college students in Taiwan, the Interdisciplinary Integration-Based Core Competencies Scale for Maternal-Infant Services (IICC-MIS scale) has been developed.

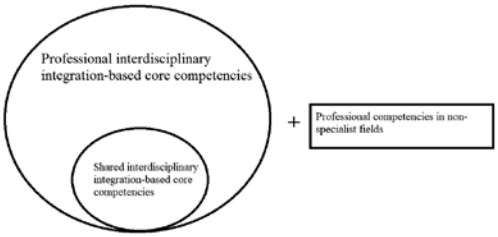

Fig3. Assessment mechanism for student interdisciplinary integration-based competencies

Although the IICC-MIS scale is designed for maternal-infant life services interdisciplinary talent cultivation, its definition of and scale for "shared interdisciplinary integration-based core competencies" can be directly used for interdisciplinary education in different professional fields since they are not related to any specific professional field.

Authors

1. Wang, T. H.*(王子華) & Yang, K.T. (http://link.springer.com/chapter/10.1007%2F978-981-10-0847-4_25)
2. Lin, C. Y. & Wang, T. H.* (王子華) (DOI: 10.12973/eurasia.2017.00657a)
3. Chen, L. C., Wang, T. H.* (王子華), Chiu, F. Y., Shen, S. Y., & Zeng, M. (DOI: 10.6173/CJSE.2017.2502.03)

Neural Correlates of Deficits in Humor Appreciation in Gelotophobics

Prof. Yu-Chen Chan
Institute of Learning Sciences and Technologies

Scientific Reports, 6, 34580 (2016)

People who have an excessive fear of being laughed at are referred to as 'gelotophobics.' Gelotophobics have social deficits in the form of relative humorlessness and heightened sensitivity to aggressive humor. The present study attempted to identify the neural substrates of responses to hostile and non-hostile jokes in gelotophobics and non-gelotophobics. Unlike gelotophobics, who are less likely to enjoy humor, particularly aggressive humor, katagelasticists, individuals who enjoy laughing at others, enjoy aggressive humor. In the present study, to focus on sensitivity or apprehension towards aggressive humor, we recruited gelotophobic and non-gelotophobic participants and excluded katagelasticists from both groups.

Gelotophobics showed greater activation than did non-gelotophobics in the *dorsal corticostriatal system*, which comprises the dorsolateral prefrontal cortex (dlPFC) and dorsal striatum, suggesting a higher degree of voluntary top-down cognitive control of emotion. As expected, gelotophobics showed less activation in the *ventral mesocorticolimbic system* (MCL) in response to both hostile and non-hostile jokes, suggesting a relative deficit in the reward system. The results support the hypothesis that MCL dysfunction in gelotophobics occurs in response to both joke types, but particularly to hostile jokes. Psychophysiological interaction (PPI) analyses further showed that gelotophobics exhibited diminished MCL activation in response to hostile jokes.

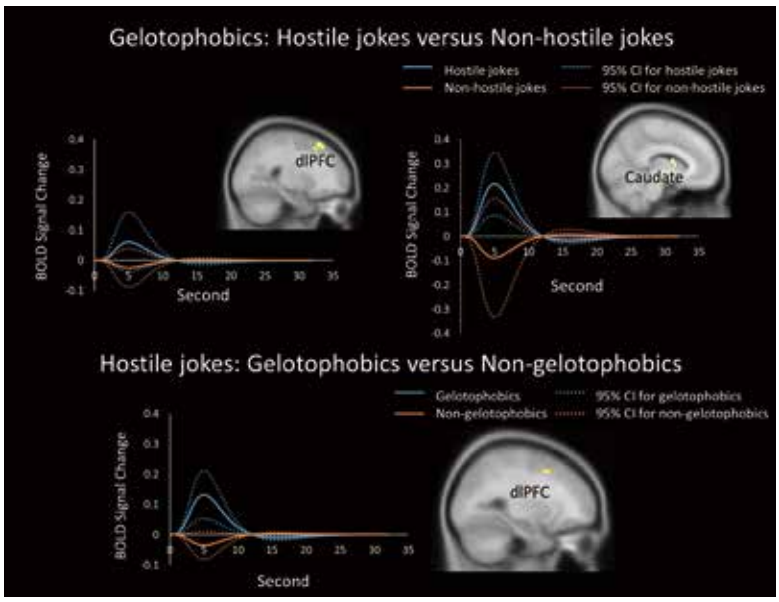

Gelotophobics responding to hostile jokes.

Results showing the time course and average BOLD signals. (Top) Differences in the mean BOLD activation within the clusters across time in response to hostile jokes (blue) versus non-hostile jokes

(orange) were found in gelotophobics in the right dorsolateral prefrontal cortex (dlPFC) and left caudate body (dorsal striatum). (Bottom) Gelotophobics (blue) showed greater activation in the left dlPFC than non-gelotophobics did (orange). The solid lines represent the evoked hemodynamic responses. The dotted lines represent the 95% confidence interval (95% CI) for the entire curve.

Conversely, non-gelotophobics displayed greater activation than gelotophobics did in the MCL system, particularly for non-hostile jokes, which suggests a more robust bottom-up emotional response. Non-gelotophobics showed greater activation in the ventral MCL reward system, which comprises the midbrain, amygdalae, nucleus accumbens (NAcc), ventral anterior cingulate cortex (vACC), and insula, particularly in response to non-hostile jokes. These group differences may have important implications for our understanding of the neural correlates of social motivation and humor appreciation.

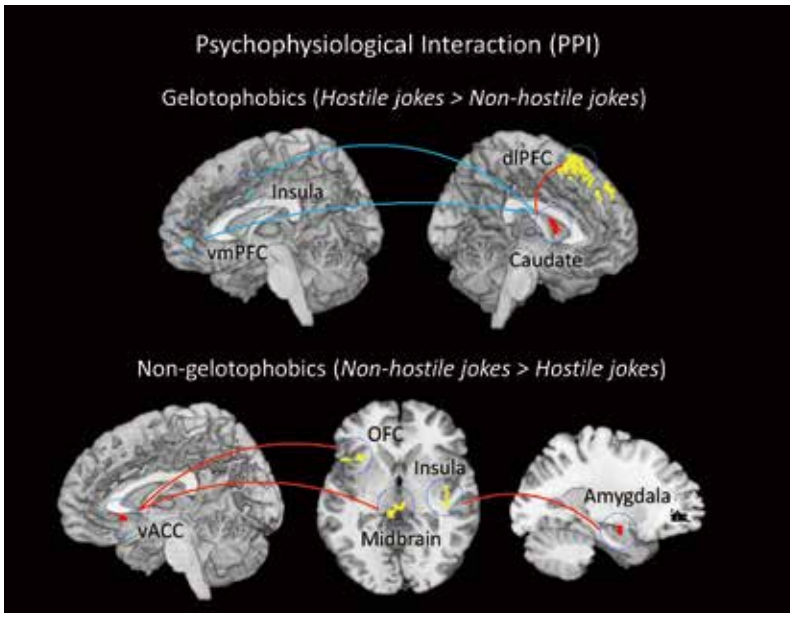

Results of the psychophysiological interaction analyses in gelotophobics and non-gelotophobics.

(Top) Gelotophobics exhibited positive functional connectivity between the left caudate (seed) and the left dorsolateral prefrontal cortex (dlPFC), and negative connectivity between the right insula and right ventromedial PFC (vmPFC) for hostile jokes versus non-hostile jokes. (Bottom) Non-gelotophobics showed positive functional connectivity between the right amygdala (seed) and the right insula and positive functional connectivity between the right ventral anterior cingulate cortex (vACC) (seed) and the left midbrain and left orbitofrontal cortex (OFC). The red regions represent the seeds including the caudate, amygdala, and vACC. A red line represents a positive interaction, whereas a blue line represents a negative interaction.

Authors

Yu-Chen Chan (詹雨臻)
https://www.nature.com/articles/srep34580

The volleyball dispenser of dynamic induction

Prof. Yun-Wen Lee
Department of Arts and Design

Quality award of the 2016 Sports Technology Innovation Design Competition

A kind of volleyball dispenser of dynamic induction, that for Training.

In the appearance design, shape it like a sports car and have a dynamic appearance. In the part of the mechanism, volleyball is shot like a bullet of air gun using ventilation of turbo fan, inhalation of volleyball, and "piston" principle, so it can withstand high strength and long practice.

The volleyball dispenser of dynamic induction, Quality award of the 2016 Sports Technology Innovation Design Competition

Authors

Yun-Wen Lee (李允文)

Exploring New Insights in Performing Chamber Repertoire with International and Taiwanese Artists at International Concert Stages

Prof. Moli Chiang
Department of Music

Every performance is a unique creation.

A pianist has to have the sensitivity and ability to adjust to the acoustics of the performance hall and instrument and the sound produced by playing partners, in order to project his/her musical ideas to the audience.

In 2016-2017, a year of chamber project, Dr. Chiang was invited to perform in international stages – Italy and Korea, as well as in Taiwan. She was first invited to perform in Taiwan National Recital Hall in Fall 2016. In May 2017, she launched her international stage appearance in Seoul, Korea, at the invitation of the Johns Hopkins University Peabody Taiwan - Korea Alumni Association. In that event, she performed Brahms Sonata No. 3 for violin and piano with the renowned violinist Ray-Chou Chang, Concertmaster of Taiwan National Symphony Orchestra. The climax of this chamber project was her well-received performance of Schumann Piano Quartet in Italy. Being one of the invited artists in the InterHarmony International Music Festival, Dr. Chiang performed in the International Artist Concert Series with three string artists from the United States - Carrie Rehkopf and John Michel, violin and cello professors from the Central Washington University, and Basil Vendryes, principal of viola from the Colorado Symphony Orchestra. Abundant new musical insights were created and shared, through collaborative and cooperative processes, among the artists. In addition, Dr. Chiang's sensitivity to the differences in performance hall acoustics, music styles and music instruments was further enhanced, an important and rewarding experience.

In concerts in Seoul and in Italy, two large romantic music compositions by Brahms and Schumann were selected to the program. Both were emotional works with a dominant role for the pianist. Prof. Chiang, as a competent pianist, displayed successfully virtuoso ability and refined sensitivity in these two demanding pieces. The performance of Schumann Piano Quartet, in Chiesa Santo Spirito, Acqui Terme,

was embraced by the large crowd of audience, who enjoyed music's hopeful and heavy-hearted expressions.

At last, Dr. Chiang's meeting and conversation with maestro Alfred Brendel, one of the greatest pianists in the world, has re-affirmed her belief in continuous exploring her international collaboration and concert appearance to strengthen and to inspire the global music community.

2017 05/28 Mozart Hall, Seoul, Korea:

Brahms Sonata No. 3 in D minor for violin and Piano (~24 min.)

2017 07/27 International Artists Series, Concert in Chiesa Santo Spirito, Acqui Terme, Italy:

Schumann Piano Quartet Op. 47 (~30 min.)

Authors

Moli Chiang (蔣茉莉), Nanette Chen, Ray Chou Chang, Carrie Rehkopf, Basil Vendryes, John Michel

https://www.youtube.com/watch?v=6tZSnQ7AyJc

https://www.interharmony.com/interharmony-concerts-italy

Joint R & D Center of Important Results

72

MediaTek-NTHU Research Center Advancing the Frontier of Future Generation Smart Mobile Devices

HIWIN-NTHU Joint Research & Development Center Focuses on Precision Machine Technologies

Prof. Cheng-Kuo Sung, Prof. Jen-Yuan Chang

"HIWIN – National Tsing Hua University (NTHU) Joint Research & Development Center," was established in 2014 at NTHU in Hsinchu, Taiwan. This joint research and development center is the largest- and longest-invested efforts in Taiwan by industry in university. It is not an exaggeration to refer it as the "Apollo moon landing program" among industry-university collaborative programs in Taiwan, as commented by Professor Hong Hocheng, the President of NTHU. Since the inauguration of the center, at least 11 Professors and more than 60 students from different departments have participated in proprietary R&D projects with budget exceeding NTD 20 Million in 2016. The center plays a unique role in developing and transforming basic science and engineering research through state-of-the-art creative engineering pathways into value-added precision components and systems that definitely can position Taiwan and HIWIN Company as the world leaders in precision intelligent machine industry. Currently, a few joint research programs are undertaking, all of which involve in-depth cross-disciplinary knowledge contents on top with solid practical experiences.

The present major R&D topics undertaken in the Center include hydrostatic bearing development, absolute magnetic encoder development and magnetic sensor technology. As an example, the R&D on precision magnetic encoders is briefly introduced herein. Magnetic encoders are mainly used in machines to detect the position of a motion stage to which they are installed. Motivated by the drawbacks of optical encoders such as high cost, unfriendly to harsh environment, etc., this research is dedicated and aimed for developing magnetic encoders to compete with optical encoders in the future marketplace. The scope ranges from design and validation of magnetic materials for realization of high-density recording, for precision magnetization for either incremental or absolute coding, for characterization of self-made magneto-resistance sensors and Hall-effect sensors as signal detection devices, which are further integrated with signal processing IC design, mechanical assembly calibration and system verification. Under the demands of machine tools manufacturers, we have designed and fabricated a linear- and a rotary-magnetic scales, which feasibility and performance have been validated through integration with linear guideways and servomotors, respectively. For example, the project led by Prof. Cheng-Kuo Sung on systemic integration has successfully demonstrated effectiveness of a direct drive motor with high resolution of rotary-magnetic encoder. The project "magnetic encoder for absolute position" led by Prof. Jen-Yuan Chang has developed a unique read head with novel algorithm for absolute positon feedback, as illustrated in Figure 1 and Figure 2, respectively. Utilizing the aforementioned precision magnetic encoders, according to the

ambitious demand goal from HIWIN to build a world-leading ultra-precision machine tool, in-depth know-how for precision components such as hydrostatic tool spindles, hydrostatic workpiece spindles, rotary hydrostatic bearing stages, linear hydrostatic bearing stages and a patented spindle mounting device enabled by magneto-rheological fluid as exampled in Figure 3 have been carefully developed and validated in the Center.

It is anticipated that with the seamless integration of the high precision components and systems, the HIWIN–NTHU Joint Research & Development Center will continue to serve as the pioneer to strengthen in-depth and in-width R&D for Taiwan and HIWIN as key player on the world stage of precision machine technologies.

Figure 1. Integration of rotary-magnetic encoder on direct drive motor.

Figure 2. Systematic platform test with integrated motor.

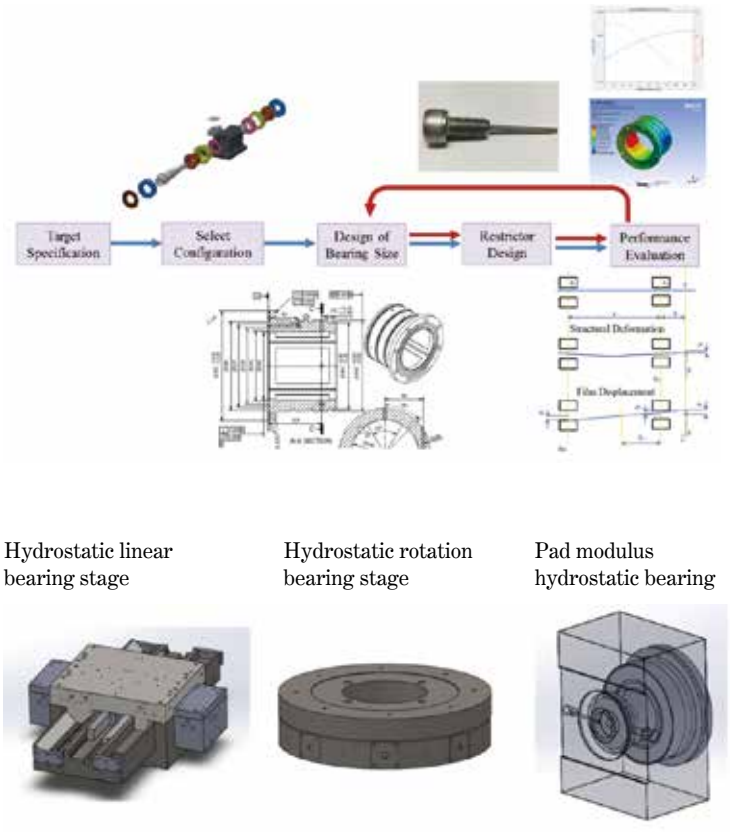

Figure 3. Examples of precision machine components and systems developed from the Center.

TSMC-NTHU Joint Research Center Focuses on Future Generation Semiconductor Devices Development

Collaborative research between TSMC and NTHU has been in the form of individual joint R&D projects (JDPs) between interested faculty members and business units of TSMC for many years. In order to integrate all JDPs with focuses on front-end integrated circuits technology development as well as attracting young talents into the semiconductor field, the Center was established in January, 2014 with a pledged annual financial support of at least NTD 15 Million from TSMC. A unique design is that 30% of the total Center budget is allocated to educate talented students in semiconductor field in the form of study allowance.

Since then, at least 30 Professors and more than 200 students from different departments have participated in the TSMC-NTHU Joint Research Center with the annual budget exceeding NTD 19.5 Million in 2017. The current major research focuses of the Center include development of advanced memory (flash, ReRAM, MRAM, etc.), investigation of FinFET beyond 16 nm technology nodes, improvement of process reliability, exploration of 2D materials, as well as CMOS/MEMS sensors for IoT applications. For example, the project led by Prof. Ya-Chin King and Chrong-Jung Lin on 'Twin-bit Via RRAM in 16nm FinFET Logic Technologies' is firstly proposed and demonstrated by 16nm standard FinFET CMOS logic platform (See Fig.1~3). The structure of the RRAM, which consists of twin resistive storage node and each one is controlled by a n-type FinFET, is shrunk to an aggressive cell size of 0.3120.346μm2 without additional mask or process step. The professors and their associates also developed a novel device for monitoring plasma induced damage in BEOL process with charge splitting capability. This device is first time proposed and demonstrated the ability to independently trace the amount as well as polarity of plasma charging effects during the manufacturing process of advanced FinFET circuits. The project "Excellent Reliability of Ferroelectric HfZrOx" led by Prof. Yung-Hsien Wu, proposed a novel NH3 plasma treatment which was employed at different HZO/TiN interfaces to investigate the impact on reliability. It is a great advance for HfO2-based FE and can be mainly attributed to significant reduction of oxygen vacancies (Vo) in HZO, especially treatment at bottom interface so that the interfacial TiOxNy which causes oxygen-deficient HZO is effectively suppressed.

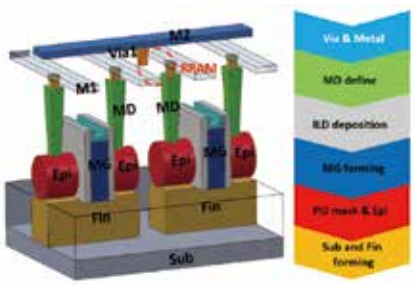

Twin-bit Via RRAM in 16nm FinFET Logic Technologies

Figure 1 (a) A 3D illustration of 1T1R Via RRAM cells implemented by the standard FinFET CMOS process. (b) Process flow of the 1T1R Via RRAM

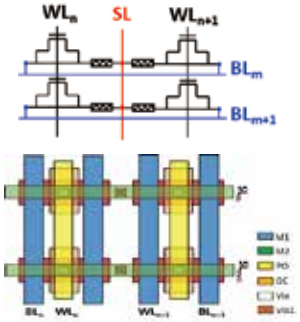

Figure 2 (a) The circuit schematic of a 2×2 NOR type array with two RRAMs sharing the same SL Via between the left and right cells. (b) 2D layout for the 2×2 array.

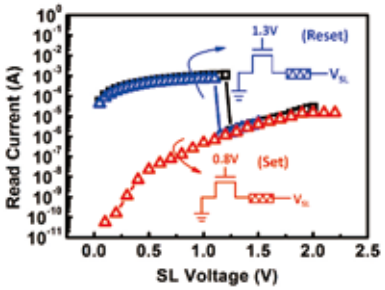

Figure 3 IV characteristics of the Via RRAM cell under unipolar DC sweep tests, revealing set/reset operations can be complete under 2.5V.

		WL	BL	SL
Set	Sel.	0.8V	0V	2V
	Unsel.	0V	Floating	0V
Reset	Sel.	1.3V	0V	1.2V
	Unsel.	0V	Floating	0V
Read	Sel.	0.6V	0V	0.6V
	Unsel.	0V	Floating	0V

Table 1 Summarize listing of the operation condition summary for the twin-bit Via RRAMs in a NOR arrays.

Charge Splitting In-situ Recorder (CSIR) for Real-time Examination of Plasma Charging Effect in FinFET BEOL Processes

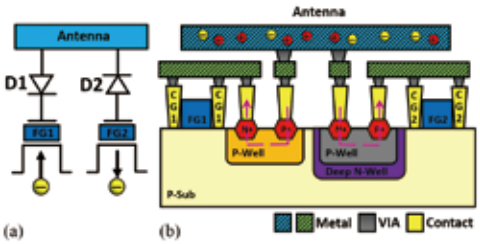

Fig.1 (a) Charge splitting in situ recorder with two separate floating gates by connecting to a forward diode (D1) and a reverse diode (D2) for detecting electron/ion charging, respectively. (b) Cross-sectional illustration of the new charge splitting in situ recorder with on-chip pn diodes, directing the positive and negative charge to the separated coupling gates, CG_1 and CG_2

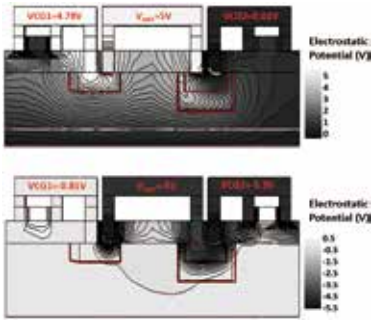

Fig.2 Simulated potential distribution in CSIR with positive and negative antenna gate voltage. The forward and reverse pn diodes successfully separate the antenna charge polarity

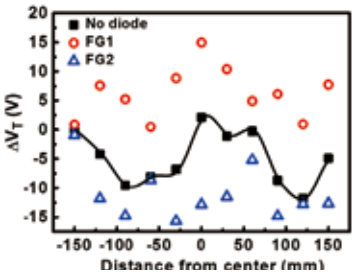

Fig.3 Distribution of delta V_T on FG_1 with forward diode and FG_2 with reverse diode, and FG without diode along the center line of a wafer

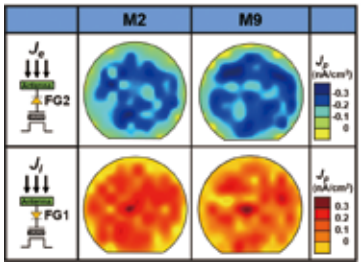

Fig.4 The projected electron and ion charging rate, J e(x,y) and J i(x,y) are obtained by the charge splitting recorders across the etching surface during metal 2 metal 9 formation

Besides research activities, the TSMC-NTHU Joint Research Center offers many scholastic activities to attract students of all grades into semiconductor related fields for advanced studies. For example, a number of sophomore and junior students are invited to join the summer Elite Camp with the opportunity to interact directly with center professors so as to inspire their interests in semiconductor research. The Center Research Project Competition offers an opportunity for students to learn semiconductors through competition among NTHU students as well as their peers at NTU, NCTU and NCKU. Above all, a sizable portion of the Center budget, over NTD 3 Million, is allocated for center students in the form of study allowance to retain excellent students to study semiconductors.

MediaTek-NTHU Research Center Advancing the Frontier of Future Generation Smart Mobile Devices

Prof. Jen-Ming Wu

Double QC-LDPC Code

The quasi-cyclic low density parity check (QC-LDPC) code has been identified as the most promising channel coding for new radio (NR) in the next generation 5G cellular system. In this work, we have developed an innovative Double QC-LDPC (DQC-LDPC) code design with parity-check matrices. The major advantages of the proposed DQC-LDPC code are:

1) flexibility in supporting low to high code rates from 1/3 to 8/9,

2) very low complexity in the encoding structure.

Double QC-LDPC code design

The DQC-LDPC is compatible to the classical QC-LDPC codes. The DQC code features double layers of circulant matrices (or circulant of circulants) as shown in Fig. 1. For convenience, "*" is used to denote the null matrix of size Q x Q. As in QC-LDPC code, each small square blocks (or submatrices) of size Q x Q are the null matrix (denoted by"*") or circulant permutation (right-shifted identity) matrices. A square collection of the small square blocks forms the outer layer of circulant matrix in H. The unique feature helps to encode the parity with double shift register array. Unlike conventional QC-LDPC encoder requires enormous matrix inverse computation, the DQC-LDPC encoder is low complexity with only shift registers and combinational logics s shown in Fig. 2. This is due to the fact that the inverse of circulant matrix is also circulant so that many of the inverse matrix operation are saves. The proposed DQC-LDPC is also flexible in supporting a wide range of code rates from 0.111 to 0.889. The work has been awarded the Taiwan and US patent in 2016 [1].

Performance evaluation

The family of DQC-LDPC code designs are illustrated in Table 1. The code rates covers from 0.111 to 0.889 with variable-degree-3. We utilize scalar min-sum decoder to evaluate the block error rate (BLER) versus SNR (Es/N0). A showcase performance results for codeword length of 256, 512,.., 4096, are shown in Fig. 2. The maximum iterations=31 with 10 soft-bits to behave as nearly-floating input. The input quantization could be further discussed in the future.

Table 1. Parameters of the proposed parity-check matrices for evaluations.

Parity	Base Codeword Length N	Flexible Codeword Length	Code Rate
256	{1280, 768, 512}	256+64*i, i in{1,2…,16}	0.5~0.8
512	{4608, 3584, 2560, 1536, 1024, 768, 640}	512+64*i, i in{1,2…,64}	0.2~0.889
768	{4864, 4096, 3072, 1792, 1280, 1024}	768+64*i, i in{1,2…,64}	0.25~0.842
1024	{5120, 4096, 3072, 2048, 1536, 1280}	1024+64*i, i in{1,2…,64}	0.2~0.8
1536	{5632, 4096, 3584, 2560, 2048}	1536+64*i, i in{1,2…,64}	0.25~0.727
2048	{6144, 5120, 4096, 3072, 2560, 2304}	2048+64*i, i in{1,2…,64}	0.111~0.667

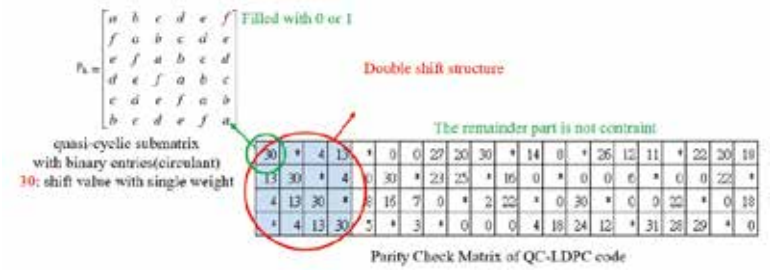

Fig. 1. Example of DQC-LDPC code features circulant of circulants submatrix

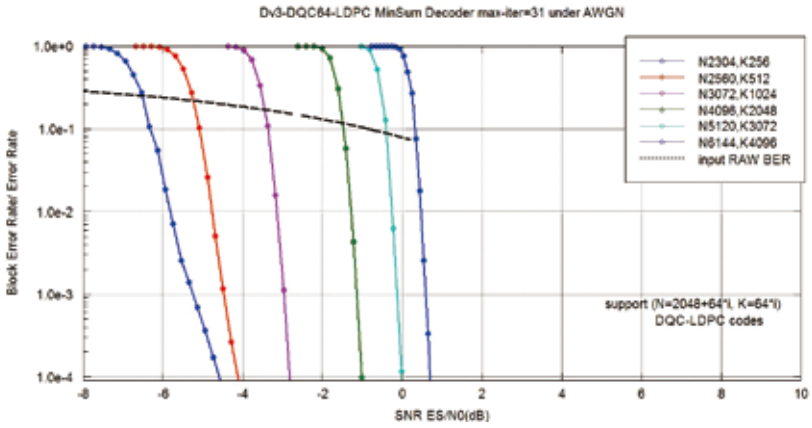

Fig. 2. Low complexity implementation of QDC-LDPC encoder

Authors

Jen-Ming Wu (吳仁銘), Sheng-Han Wu
http://www.google.com/patents/US20140298132

Research Highlights

Engineering and Applied Sciences

The Penetrated Delivery of Drug and Energy to Tumors by Lipo-graphene Nanosponges for Photolytic Therapy
Prof. Shang-Hsiu Hu

3D TCAD Simulation for CMOS Nanoeletronic Devices
Prof. Yung-Chun Wu

Angiogenesis-targeting Microbubbles Combined with Ultrasound-Mediated Gene Therapy in Brain Tumors
Prof. Chih-Kuang Yeh

Cluster analysis
Prof. Yen-Chang Chang

Left ventricular regional myocardial motion and twist function in repaired tetralogy of Fallot evaluated by magnetic resonance tissue phase mapping
Prof. Hsu-Hsia Peng

Humanities and Social Sciences

Melodic intonation therapy as an effective facilitator of language function recovery: A DTI study in people with non-fluent aphasia
Prof. Fan-Pei Gloria Yang

Historical Writing in the Song dynasty
Prof. Cho-ying Li

Chinese Art History, Images of War, Qing Court Art
Prof. Ya-chen Ma

Mobility, labour, learning, gender, economy
Prof. I-Chieh Fang

Engineering and Applied Sciences

▼ The Penetrated Delivery of Drug and Energy to Tumors by Lipo-graphene Nanosponges for Photolytic Therapy

Prof. Shang-Hsiu Hu
Department of Biomedical Engineering and Environmental Sciences

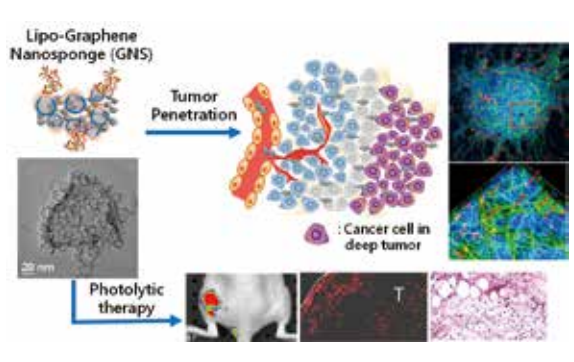

Delivery of drug and energy within responsive carriers that effectively target and accumulate in cancer cells promise to mitigate side effects and to enhance the uniquely therapeutic efficacy demanded for personalized medicine. To achieve this goal, however, these carriers which are usually piled up at the tumors periphery near the blood vessels must simultaneously overcome the challenges in low tumor penetration and transport sufficient cargos to the deep tumor to eradicate whole cancer cells. Here, we report a sponge-like carbon material on graphene nanosheet (graphene nanosponge)-supported lipid bilayers (lipo-GNS) that doubles as a photothermal agent and high cargo payload platform, which releases a burst of drug/energy (docetaxel (DTX) and gasified perfluorohexane (PFH)) and intense heat upon near-infrared irradiation. Ultrasmall lipo-GNS (40 nm) modified with a tumor targeting protein that penetrates the tumor spheroids through transcytosis exhibited a 200-fold increase in accumulation than a 270 nm variant of the lipo-GNS. Furthermore, a combination of therapeutic agents (DTX and PFH) delivered by lipo-GNS deep into tumors was gasified and released into the tumor spheroids, and successfully ruptured and suppressed xenograft tumors in 16 days without distal harm when subjected to a single 10 min near infrared (NIR) laser treatment. This sophisticated lipo-GNS is an excellent delivery platform for penetrated, photo-responsive, and combined gasification/chemo-thermotherapy to facilitate tumor treatment and for use in other biological applications.

http://pubs.acs.org/doi/abs/10.1021/acsnano.6b04414
http://onlinelibrary.wiley.com/doi/10.1002/adfm.201700056/full
http://www.sciencedirect.com/science/article/pii/S0169409X1630182X

▼ 3D TCAD Simulation for CMOS Nanoeletronic Devices

Prof. Yung-Chun Wu
Department of Engineering and System Sciences

This book demonstrates how to use the Synopsys Sentaurus TCAD 2014 version for the design and simulation of 3D CMOS (complementary metal–oxide–semiconductor) semiconductor nanoelectronic devices, while also providing selected source codes (Technology Computer-Aided Design, TCAD). Instead of the built-in examples of Sentaurus TCAD 2014, the practical cases presented here, based on years of teaching and research experience, are used to interpret and analyze simulation results of the physical and electrical properties of designed 3D CMOSFET (metal–oxide–semiconductor field-effect transistor) nanoelectronic devices, including Si, Ge, InGaAs FinFET, GAA NWFET, junctionless FinFET, tunnel FinFET. In final chapter, also predicts the feasible options for Si and Ge FinET of ultimate Lg=3nm minimum dimensions.

http://www.springer.com/gp/book/9789811030659
https://www.amazon.com/TCAD-Simulation-CMOS-Nanoeletronic-Devices/dp/9811030650

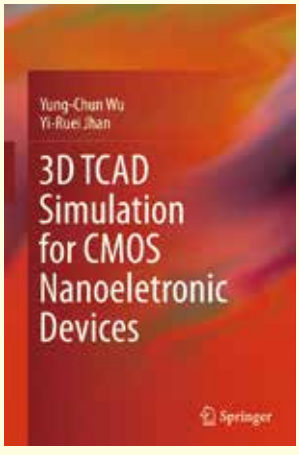

▼ Angiogenesis-targeting Microbubbles Combined with Ultrasound-Mediated Gene Therapy in Brain Tumors

Prof. Chih-Kuang Yeh
Department of Biomedical Engineering and Environmental Sciences

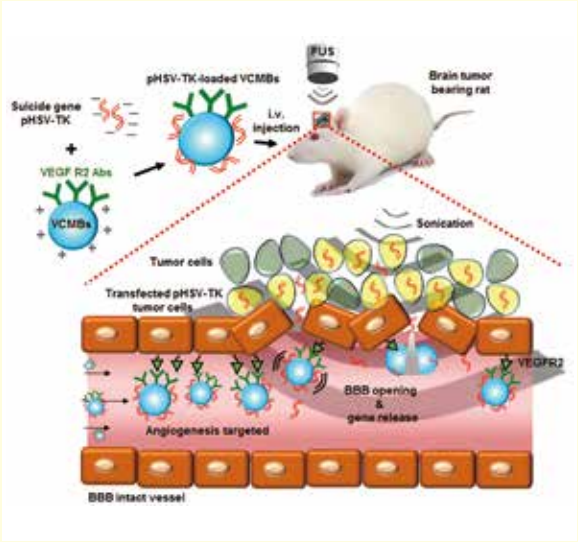

Fig1. The overall experiment schematic diagram. The angiogenesis-targeting DNA loaded microbubbles combined with ultrasound for gene delivery in brain tumor.

The major challenges in gene therapy for brain cancer are poor transgene expression due to the blood-brain barrier (BBB) and neurologic damage caused by conventional intracerebral injection. Non-viral gene delivery using ultrasound-targeted microbubble (MB) oscillation via the systematic transvascular route is attractive, but there is currently no high-yielding and targeted gene expression method. In this study, we developed a non-viral and angiogenesis-targeting gene delivery approach for efficient brain tumor gene therapy without brain damage. We developed a VEGFR2-targeted and cationic microbubble (VCMB) gene vector for use with transcranial focused ultrasound (FUS) exposure to allow transient gene delivery. The system was tested in a brain tumor model using the firefly luciferase gene and herpes simplex virus type 1 thymidine kinase/ ganciclovir (pHSV-TK/ GCV) with VCMBs under FUS exposure for transgene expression and anti-tumor effect. In vitro data showed that VCMBs have a high DNA-loading efficiency and high affinity for cancer cells. In vivo data confirmed that this technique enhanced gene delivery into tumor tissues without affecting normal brain tissues. The VCMB group resulted in higher luciferase expression (3.8 fold) relative to the CMB group (1.9 fold), and the direct injection group. The tumor volume on day 25 was significantly smaller in rats treated with the pHSV-TK/GCV system using VCMBs under FUS (9.7 ± 5.2 mm3) than in the direct injection group (40.1 ± 4.3 mm3). We demonstrated the successful use of DNA-loaded VCMBs and FUS for non-viral, noninvasive and targeted gene delivery to brain tumors.
https://www.ncbi.nlm.nih.gov/pubmed/?term=Angiogenesis-targeting+Microbubbles+Combined+with+Ultrasound-Mediated+Gene+Therapy+in+Brain+Tumors

▼ Cluster analysis

Prof. Yen-Chang Chang
Center for General Education

A robust automatic clustering algorithm for probability density functions with application to categorizing color images

This study develops a robust automatic algorithm for clustering probability density functions based on the previous research. Unlike other existing methods that often pre-determine the number of clusters, this method can self-organize data groups based on the original data structure. The proposed clustering method is also robust in regards to noise. Three examples of synthetic data and a real-world COREL dataset are utilized to illustrate the accurateness and effectiveness of the proposed approach.

▼ Left ventricular regional myocardial motion and twist function in repaired tetralogy of Fallot evaluated by magnetic resonance tissue phase mapping

Prof. Hsu-Hsia Peng
Department of Biomedical Engineering and Environmental Sciences

Objectives: We aimed to characterise regional myocardial motion and twist function in the left ventricles (LV) in patients with repaired tetralogy of Fallot (rTOF) and preserved LV global function.

Methods: We recruited 47 rTOF patients and 38 age-matched normal volunteers. Tissue phase mapping (TPM) was performed for evaluating the LV myocardial velocity in longitudinal, radial, and circumferential (Vz, Vr, and VØ) directions in basal, middle, and apical slices. The VØ peak-to-peak (PTP) during systolic phases, the rotation angle of each slice, and VØ inconsistency were computed for evaluating LV twist function and VØ dyssynchrony.

Results: As compared to the controls, the rTOF patients presented decreased RV ejection fraction (RVEF) ($p = 0.002$) and preserved global LV ejection fraction (LVEF). They also demonstrated decreased systolic and diastolic Vz in several LV segments and higher diastolic Vr in the septum (all $p < 0.05$). A lower VØ PTP, higher VØ inconsistency, and reduced peak net rotation angle (all $p < 0.05$) were observed. The aforementioned indices demonstrated an altered LV twist function in rTOF patients in an early disease stage.

Conclusions: MRTPM could provide information about early abnormalities of LV regional motion and twist function in rTOF patients with preserved LV global function.

https://www.ncbi.nlm.nih.gov/pubmed/28677054

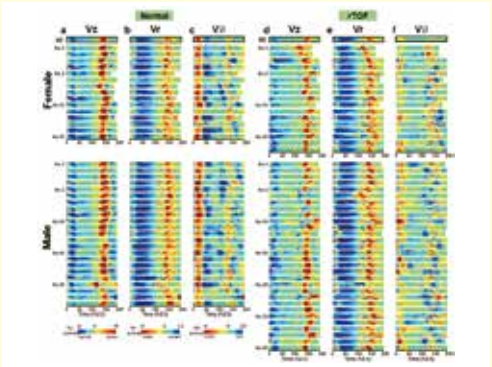

Fig. 1. Colour plots of the segmental dynamic evolution of the LV velocity in the basal slice. The dynamic evolutions of the Vz, Vr, and VØ of the 6 segments in the basal slice of the normal volunteers (a-c) and rTOF patients (d-f) are shown. The upper and lower panels represent female and male groups, respectively. The mean velocities of all subjects, denoted by black lines, are shown on the top of each panel. The colour bars indicate the directions and scales of the 3 velocities, respectively.

Humanities and Social Sciences

▼ Melodic intonation therapy as an effective facilitator of language function recovery: A DTI study in people with non-fluent aphasia

Prof. Fan-Pei Gloria Yang
Department of Foreign Languages and Literature

In order to constructing appropriate response for articulation, the dorsal and ventral streams interact with each other for speech recovery.

The results confirmed that, comparing to the control participants, people with non-fluent aphasia demonstrated decreased FA, which is associated to negative change of WM connectivity. Compared to the non-MIT group, all participants in the MIT group showed not only improved sentence production but also increased FA in the WM tracts. Further, positive correlations between the language performance and FA values were found in the two language-related dorsal stream in the right hemisphere, right-AF and right-SLF. As the primary language pathway, AF connects Wernicke's and Broca's area, whilst SLF is linked to sound to motor mapping. Although the tracts (IFOF, ILF, and UF) located in the ventral stream did not significantly correlate with the language performance, positive response towards MIT was observed.

http://www.frontiersin.org/10.3389/conf.fpsyg.2016.68.00122/event_abstract

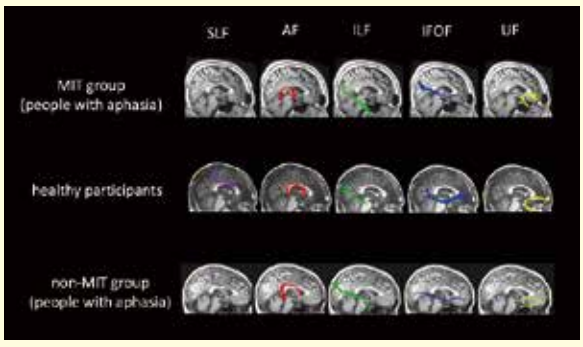

▼ Historical Writing in the Song dynasty

Prof. Cho-ying Li
Institute of History

Both articles discuss the historical writing in the Song dynasty and its significances.

1. Chen Dong, a student at the Imperial University in Kaifeng, was executed in 1127 because he criticized Song policy to relocate to the south rather than continue military resistance against the Jurchen invasions. The historical process that transformed an executed criminal into one of the seminal moral voices of Song history reveals the tension between literati governance and autocratic governance throughout the dynasty. Thirty-eight colophons, dating 1222–1259, which were written on a holograph memorial from the day of Chen's execution, demonstrate how literati resistance to the administrations of Shi Miyuan and his nephew Shi Songzhi, especially among adherents of the "learning of the Way" movement, enhanced the historical stature of Chen Dong and presented him as a voice of "public opinion" against the autocratic power of higher authority.

2. The Records of The Five Dynasties, compiled by Xue Juzheng and his colleagues, provided an official understanding of the history of this period but did not prevent early Song scholars from composing other texts regarding that period of division. Because these scholars saw incompleteness caused by a lack of materials and historians' incompetence as major flaws in the Records of The Five Dynasties, they maintained it was necessary to correct such flaws by supplementing the official history with hearsay evidence, ranging from witnesses' testimonies to diviners' predictions. This article argues that this supplementation was not merely an effort to offer more information, but an action to demonstrate specific political views. Two books under discussion in this article – Wudaishi quewen (missing texts of five dynasties history) by Wang Yucheng and Wudaishi bu (supplement to the history of the five dynasties) by Tao Yue – illuminate this point: Wang selected hearsay evidence to highlight the cultural and political achievements of the Song dynasty, and Tao used auspicious and ominous rumors to challenge the idea of a linear and singular transmission of the mandate of heaven upheld by the Song court. In turn, Ouyang Xiu and Yin Zhu, who benefited from their experience in Qian Weiyan's circle where rich information about previous political authorities circulated, decided to participate in this trend of rewriting five dynasties' history. Ouyang's experiences in guan'ge (three institutes and imperial library) later changed his attitude toward hearsay evidence: He would omit it while seeking appropriate guidelines to write a new history of the five dynasties. Finally, this article argues that Ouyang and Yin's plan to co-author this new history eventually failed because of Yin's unfortunate political career and their disagreement over historiographical issues.

▼ Chinese Art History, Images of War, Qing Court Art

Prof. Ya-chen Ma
Institute of History

By tracing the history of commemorative images of war, the book, T*he Commemorative Images of War: The Cultural Construction of Qing Martial Prowess*, reveals the underresearched popularity of visual culture among officials in the Ming dynasty and demonstrates how the Manchu monarchs gradually transformed the visual culture of Ming elites to assert the cultural hegemony of the imperial Qing. Both Sinicization and "the New Qing History" agree that the adaption of Chinese political traditions was crucial to the Manchu domination over China proper. Nonetheless, this book argues that the Manchu court actively and effectively constructed its cultural dominance over the ruled Han subjects by another mechanism. That is the cultural hegemony of the imperial Qing in which the Manchu court appropriated the trendy cultural practices of Han Chinese elites, including the visual culture of scholar-officials, to maintain its cultural supremacy over China proper.

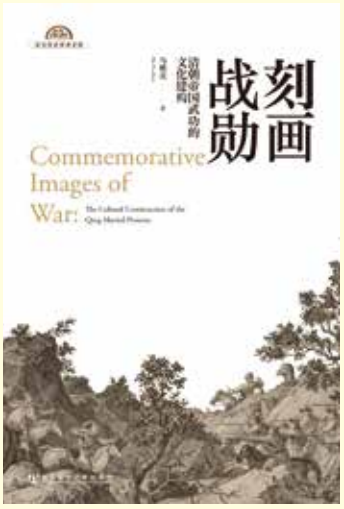

▼ Mobility, labour, learning, gender, economy

Prof. I-Chieh Fang
Institute of Anthropology

Fang, I-C. (2017) 非正式標準化與道德經濟 [The informal standardisation and moral economy]。台灣人類學刊 [Taiwan Journal of Anthropology] 15(1): 103-166. (TSSCI)

Fang, I-C. (2017) "Kajanus, Anni. 2015. Chinese student migration, gender and family. Basingstoke, New York: Palgrave Macmillan. 194 pp. Hb.: US$74.99. ISBN: 9781137509093." Social Anthropology/ Anthropologie Sociale 25(2): 261-262.

Fang, I-C. (2017, accepted) Precarity, guanxi and the informal economy of peasant workers in contemporary China. In Industrial Labor On the Margins of Capitalism: Precarity, Class and the Neoliberal Subject, eds. C. Hann and J. Parry. Oxford, New York: Berghahn.

Fang, I-C. (2016) Independent, Yet Not Grown Up': Young Migrant Workers' Journey in Post-Mao China. In Child Poverty, Youth (Un)Employment, and Social Inclusion, eds. Maria Petmesidou; Delamonica, Enrique; Henry-Lee, Aldrie & Papatheodorou, Christos. Pp. 263-292. Stuttgart: *Ibidem*-Verlag.

方怡潔 (2016) 市場化的青春：青春作為中介移民打工的社會機制 [The marketised adolescence: when the adolescence becomes the mediating mechanism for structural discrimination and social inequality]。考古人類學刊 [Journal of Archaeology and Anthropology] 84: 111-144。(TSSCI)

2016-2017 R&D REPORT

Office of Research and Development
National Tsing Hua University

No. 101, Section 2, Kuang-Fu Road,
Hsinchu, Taiwan 30013, R.O.C.
Tel : +886-3-571-7470
http://rdweb.nthu.edu.tw/Default.aspx
http://rdweb.nthu.edu.tw/English/English.aspx

National Tsing Hua University
No. 101, Section 2, Kuang-Fu Road, Hsinchu, Taiwan 30013, R.O.C.
Tel : +886-3-571-5131
http://www.nthu.edu.tw